

A3707421

CLOUD CHEMISTRY OF HALOGEN FORMATION FINAL REPORT  
DDO Work Unit 311B, OGA, February 15, 1970

# Gulf General Atomic Incorporated

GA-9987  
Work Unit 311B

## CLOUD CHEMISTRY OF HALOGEN FORMATION

### FINAL REPORT

by

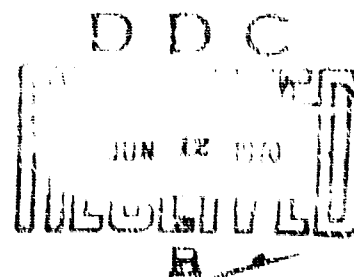
J. R. Norman and P. Winchell

for

Office of Civil Defense  
Office of the Secretary of the Army  
Washington, D. C. 20310

under

Contract DAKC20-69-C-0138

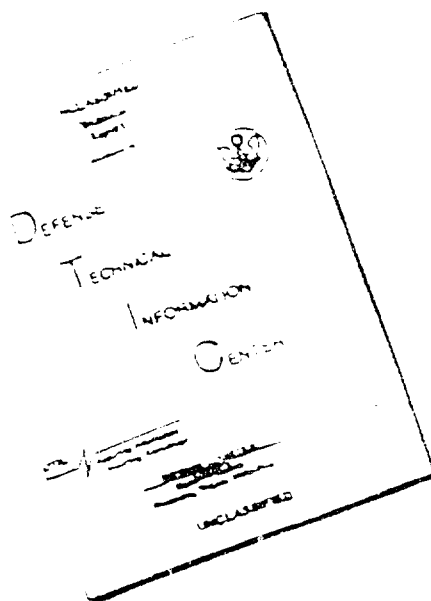


This document has been approved for public release  
and sale; its distribution is unlimited.

February 15, 1970

65

# DISCLAIMER NOTICE



THIS DOCUMENT IS BEST  
QUALITY AVAILABLE. THE COPY  
FURNISHED TO DTIC CONTAINED  
A SIGNIFICANT NUMBER OF  
PAGES WHICH DO NOT  
REPRODUCE LEGIBLY.

REPRODUCED FROM  
BEST AVAILABLE COPY

THIS DOCUMENT CONTAINED  
BLANK PAGES THAT HAVE  
BEEN DELETED

# **Gulf General Atomic**

Incorporated

P.O. Box 608, San Diego, California 92112

GA-9945  
Work Unit 311B

## **CLOUD CHEMISTRY OF FALLOUT FORMATION FINAL REPORT**

**Work done by:**

E. E. Anderson  
J. M. Dixon  
J. H. Norman  
J. N. Smith, Jr.  
H. G. Staley  
P. Winchell

**Report written by:**

J. H. Norman  
P. Winchell

for  
Office of Civil Defense  
Office of the Secretary of the Army  
Washington, D.C. 20310

under  
Contract DAHC20-69-C-0138

### **OCD REVIEW NOTICE**

This report has been reviewed in the Office of Civil Defense and approved for publication. Approval does not signify that the contents necessarily reflect the views and policies of the Office of Civil Defense.

This document has been approved for public release and sale; its distribution is unlimited.

CLOUD CHEMISTRY OF FALLOUT FORMATION FINAL REPORT

by

J. H. Norman and P. Winchell

Gulf General Atomic Incorporated Report GA-9945

February 15, 1970

Prepared for Office of Civil Defense under Contract

DAH20-69-C-0138, Work Unit 3118

SUMMARY

In initial studies of short-lived fission products for use in fallout fractionation models, several known isotopes have been recognized. The observed gamma ray intensities of recognized energies from the double-tape recoil-range measuring system are consistent with expected recoil range variations. It is planned to satisfy a requirement for more intense gamma spectra by moving the recoil fission product source close to the reactor.

The interaction between condensation phenomena and gas- and condensed-phase diffusion of fission products during fallout formation has been investigated analytically. Regions of importance of each of these phenomena have been discussed.

Further tests of the application of the compensation law to condensed-state diffusion data have been carried out. The compensation law - reciprocal ionic radius relationships applied well to all silicate systems except those loaded by fission-product recoil.

The thermodynamics of  $\text{CoO}_2(\text{g})$  have been measured. Attempts to define the stabilities of  $\text{AsO}_2(\text{g})$  and  $\text{SnO}_2(\text{g})$  have failed because of low stability of these species.

Gaseous release of iodine from  $\text{TeO}_2$  particles has been shown to be controlled by diffusion in the  $\text{TeO}_2$ . Rates of diffusion have been determined. These data indicate that the volatility of iodine from fallout particles could be very high. Leaching studies of recoil loaded fission products are consistent with release of these fission products to the aqueous leaching solution being diffusion controlled. These measurements point out the importance of the distributions of fission products in fallout particles to their biological activities.

## CONTENTS

SUMMARY . . . . .	111
INTRODUCTION . . . . .	1
SHORT-LIVED FISSION PRODUCT STUDIES . . . . .	3
APPARATUS, INSTRUMENTATION, AND METHODS . . . . .	3
EXPERIMENTAL RESULTS . . . . .	9
FISSION PRODUCT SORPTION RATE MECHANISMS . . . . .	18
EXPERIMENTAL CONDENSATION COEFFICIENT STUDIES . . . . .	25
DIFFUSION OF RADIOACTIVE NUCLIDES IN MOLTEN SILICATES . . . . .	26
THERMODYNAMICS OF FISSION PRODUCT OXIDE SYSTEMS BY MASS SPECTROMETRY . . . . .	35
REVISED HENRY'S LAW CONSTANT VALUES . . . . .	38
RELEASE OF RADIOIODINE BY SIMULATED FALLOUT PARTICLES . . . . .	40
LEACHING STUDIES . . . . .	50
PUBLICATIONS . . . . .	54
REFERENCES . . . . .	55

## FIGURES

1. Simplified diagram of tape processing assembly . . . . .	4
2. Tape processing assembly . . . . .	5
3. Fission-product recoil-range parameter $C_3/C_2$ in Mylar vs. atomic mass. Data taken from Ref. 1 . . . . .	7
4. Part of spectrum from the moving tape adjacent to the source. Curves are smoothed data . . . . .	12
5. Part of spectrum from the moving tape furthest from the source. Curves are smoothed data . . . . .	14
6. Fractional sorptions as a function of time for varying values of $rh$ . . . . .	21

FIGURES (continued)

7. Fractional sorptions as a function of time for varying values of rh, showing regions of gas-phase diffusion and condensed-state diffusion control . . . . .	23
8. Diffusion coefficients for transport of radiocesium in molten media of albite composition as a function of temperature . . . . .	27
9. Self-diffusion coefficient of Na-24 and viscosity as functions of temperature for NBS Standard Glass No. 710 . . . . .	30
10. Concentration profiles for simultaneous diffusion of radio-nuclides in 1450°K CaO-A <sub>2</sub> O <sub>3</sub> -SiO <sub>2</sub> eutectic at 1601°K . . . . .	34
11. Apparatus used for monitoring the release of radioiodine by simulated fallout particles . . . . .	41
12. Fractional release F of I-131 by neutron-irradiated TeO <sub>2</sub> particles as a function of the square root of the time at four temperatures . . . . .	42
13. Dependence of estimated diffusion coefficients upon temperature for release of radioiodine from neutron-irradiated TeO <sub>2</sub> particles . . . . .	44
14. Calculated fractional release F of radioiodine by an 0.1 μm particle at 298°K . . . . .	46
15. Fractional release of surface-adsorbed I-131 by glass spheres at 298°K in laboratory air as a function of time . . . . .	47
16. Leaching of adsorbed I-131 from glass spheres with distilled water and potassium iodide at 298°K as a function of time . . . . .	49
17. Fractional release of fission products from eutectic glass during leaching; the average uncertainty is 15% . . . . .	51
18. Fractional release of fission products from Nevada glass during leaching; the average uncertainty is 25% . . . . .	52

TABLES

1. A list of prominent peaks in spectrum from tape adjacent to source in the 60-min experiment with delay time of 4.0 sec . . . . .	10
2. Prominent peaks in spectra from two tapes for the 240-min experiment with a delay time of 23 sec . . . . .	11
3. Additional peaks from 240-min experiment for tape adjacent to source (energies in keV) . . . . .	16
4. Diffusion coefficients for transport of radiocesium in molten media of albite composition . . . . .	26
5. Arrhenius parameters for diffusion in melts of albite composition . . . . .	28

TABLES (continued)

6. Diffusion coefficients for transport of Na-24 in NBS-710 glass. . .	29
7. Radii at various temperatures using Equation (13) and experimental diffusivity and viscosity data . . . . .	31
8. Results of pressure calibrations and $\Delta S_T^0$ calculations for reaction (Eq. 17) . . . . .	37
9. Revised Henry's law constants . . . . .	39
10. Diffusion coefficients for radioiodine release by simulated fallout particles . . . . .	43
11. Radionuclides present in leaching slurries for Nevada and eutectic glasses . . . . .	53

## INTRODUCTION

In the cloud chemistry program carried out at Gulf General Atomic Incorporated during the past year, there has been a shift in emphasis toward studies of short-lived fission products. The effort in the short-lived fission product study has been principally one of preparing for accumulation of precise data. In our last final report (Ref. 1), we described a unique method of obtaining the desired half-life data. This was demonstrated by making studies more than one-half hour after fission. During the present reporting period, we assembled the equipment to perform these studies in the desired time range (1 to 100 sec after fission). We have obtained some data in this time range. The one problem was that of having a weak fission source. In spite of this, over 30 gamma transitions have been recognized. The estimated recoil ranges of the source nuclides, whose transitions are reasonably well documented by other workers, provide encouragement for the success of these studies. During a follow-on program, we intend to obtain orders-of-magnitude more accurate transition intensity data by placing the recoil fission product source adjacent to a graphite thermal column, which, in turn, is fed neutrons by a Gulf General Atomic TRIGA reactor. We expect that this system will provide the data required for these studies.

As a continuation of our diffusion studies, we have attempted to study the diffusion of recoil loaded fission products in several silicates. The results of these studies were enigmatic in that the coefficients measured for various fission products exhibit little variation with diffusing species. In our other diffusion studies, diffusion coefficients were definitely dependent on the diffusing species (i.e., the element considered) except at the cross-over temperature predicted by the compensation law. Other diffusion studies included in this report can still be described using the compensation law - reciprocal ionic radius relationships.

An analysis of sorption of fission products during fallout formation, as governed by condensation coefficients, condensed-phase diffusion coefficients, and gas-phase diffusion coefficients, has been made. This work extends the analysis presented in the last final report (Ref. 1) to include different sorption regimes and gas-phase diffusion. The discussion outlines the anticipated behavior of systems in fallout with respect to values of the three important parameters.

An experimental study has demonstrated some of the problems in obtaining appropriate experimental condensation coefficients. It has long been known that the condition of the surface is extremely important in determining condensation coefficients. The importance of this condition was emphasized by the observation of cosine law scattering of noble gases from hot molten glass surfaces. Specular scattering would have indicated a low condensation coefficient for these gases. Cosine law scattering indicates either a long residence time on the surface or a rough surface. We prefer to believe that our observations indicate a surface roughened by gas adsorption rather than the long residence time on the surface, which implies a condensation coefficient near unity.

The other fallout studies reported here include (1) a mass spectrometrically derived description of the stability of  $\text{GeO}_2(\text{g})$ , (2) an updating of reported Henry's law constants, (3) a description of the "leaching" of iodine from particulate matter by hot, moist air, and (4) a description of the leaching of recoiled fission products from glasses using aqueous techniques.

## SHORT-LIVED FISSION PRODUCT STUDIES

Half-life data on short-lived fission products are needed to serve as input to fallout models so that the fission product isotopes, which are present during the cooling of a nuclear cloud, are described quantitatively as a function of time. We have initiated short-lived fission product studies using a steady-state system for evaluating these half-lives. The first step toward accomplishing this goal was to design an experimental apparatus which would allow us to achieve precise, meaningful steady-state gamma ray intensity data. The main requirement, that of obtaining time-independent data (i.e., steady-state data), is for a separation of nascent fission fragments from fissioning material. We have selected the property of fission product recoil to accomplish this separation. In addition to providing the separation, this property also affords information concerning the fission products themselves, since recoil ranges are quite dependent on the properties of the recoiling fission products. Generally, the recoil range and half-life data can be obtained from the mechanically separated recoiled fission products using a moving tape system.

## APPARATUS, INSTRUMENTATION, AND METHODS

A simplified diagram and a photograph of the tape system are shown in Figs. 1 and 2. Two Mylar tapes, 2 in. by approximately 6 micrometers, move from supply reels past a thermal-neutron irradiated, enriched-uranium source and then through a series of rollers and capstans, which separate the two tapes. Each tape is then passed several times across the face of a lithium-drifted germanium detector on the way to a take-up reel. Tapes can be threaded so that they give either equal delay times or so that both detectors monitor a single tape with different delay times for half-life determinations. The apparatus, designed at Gulf General Atomic, was fabricated by Almond Instruments Company of Covina, California. The detectors were obtained from Princeton Gamma Tech, Inc., and have a resolution of better than 2.5 keV for

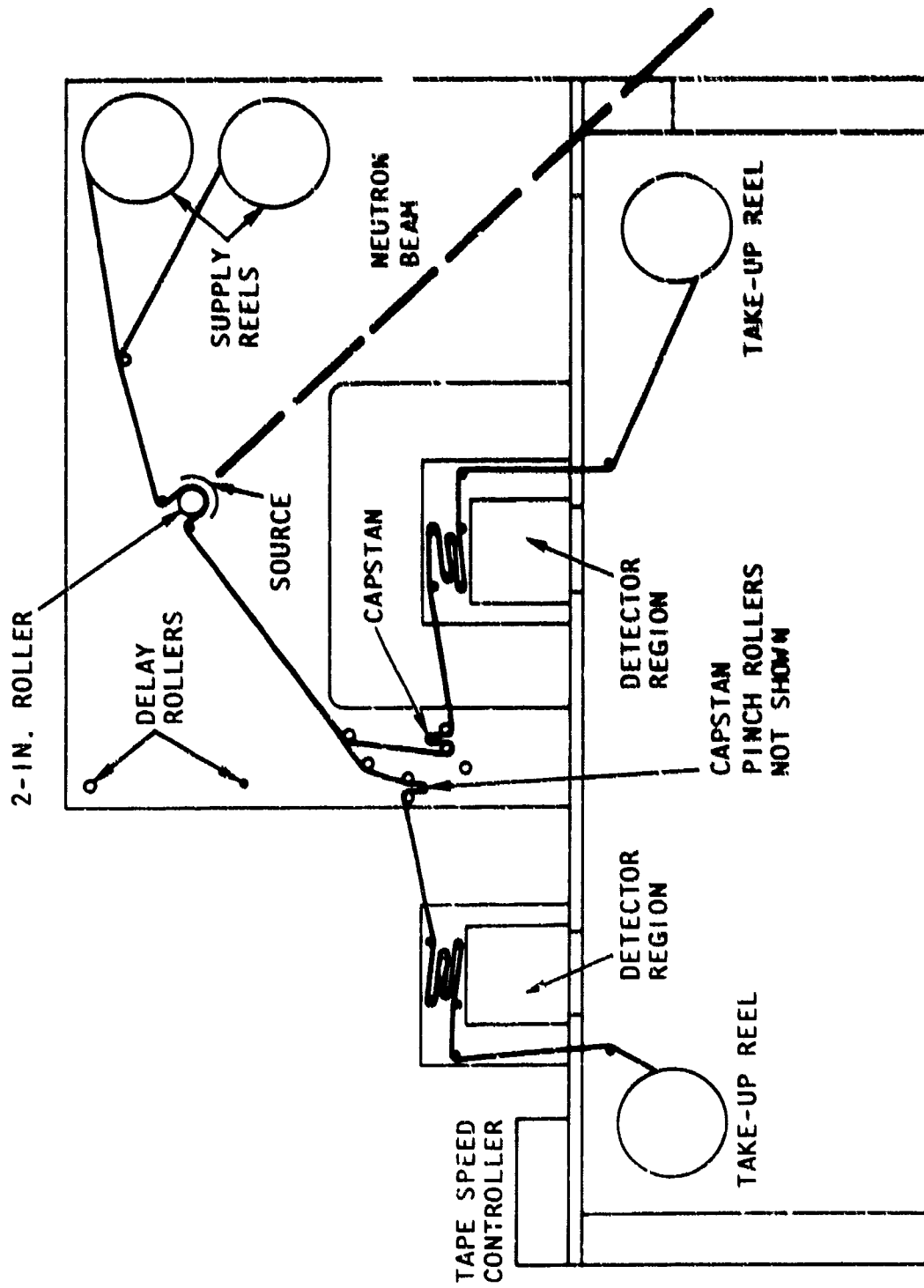


Fig. 1. Simplified diagram of tape processing assembly



T78795

Fig. 2. Tape processing assembly

the 1333-keV, Co-60 gamma ray spectral peak (width at half-maximum intensity) with an efficiency 8% of that exhibited by a 3 in. by 3 in. sodium iodide crystal for this gamma ray, both at 25 cm. Signals from the detectors are amplified by Canberra pre-amplifiers and amplifiers and fed into a TMC 4096-channel analyser, which can be operated as a 2048-channel analyser for each detector. Two detectors are employed so that accurate recoil range measurements can be made. The principle of the experiment is that fission products are recoiled from the source through a 6-micrometer Mylar source covering tape into the two moving 6-micrometer tapes. For a particular photopeak, the ratio of the integrated signals from the identically delayed moving tapes is a function of the recoil range of the nuclide, which, in turn, can be related empirically to the atomic mass of the nuclide. Thus, atomic mass data are obtained for nuclides causing observed photopeaks. This is illustrated in Fig. 3 where the data were obtained with a static system (Ref. 1). Then, a single tape is studied with the two detectors at different delay times to obtain the "decay curves" establishing the half-lives of the observed nuclides.

The employed highly thermalized, well-collimated neutron beam had a flux of  $6 \times 10^5$  n/cm<sup>2</sup>-sec at the target. The beam was conducted through a 30-ft beam tube closely associated with a graphite thermal column adjacent to the Mark III Gulf General Atomic TRIGA reactor, which was operated at 900 kW. Shielding with boronated water, boronated paraffin, and lead bricks was provided around the exit flange of the beam tube. Detector shielding was accomplished with these materials and lithium carbonate. The beam impinged on the back side of the source holder, which was half of a right-circular cylinder made of 1/16-in., 6061 aluminum. The source area was 4 in.<sup>2</sup>. The low neutron flux was found to be the limiting factor in these experiments.

Some difficulty was encountered in preparing the uranium source; therefore, natural uranium was used for trial preparations. Attempts to electroplate uranium onto platinum, using a buffered nitrate-oxalate solution and other standard methods (Ref. 2), failed because the amount of uranium adhering was insufficient for our purpose. Attempts at vapor deposition of uranium metal onto aluminum, using a uranium-coated tungsten filament, also

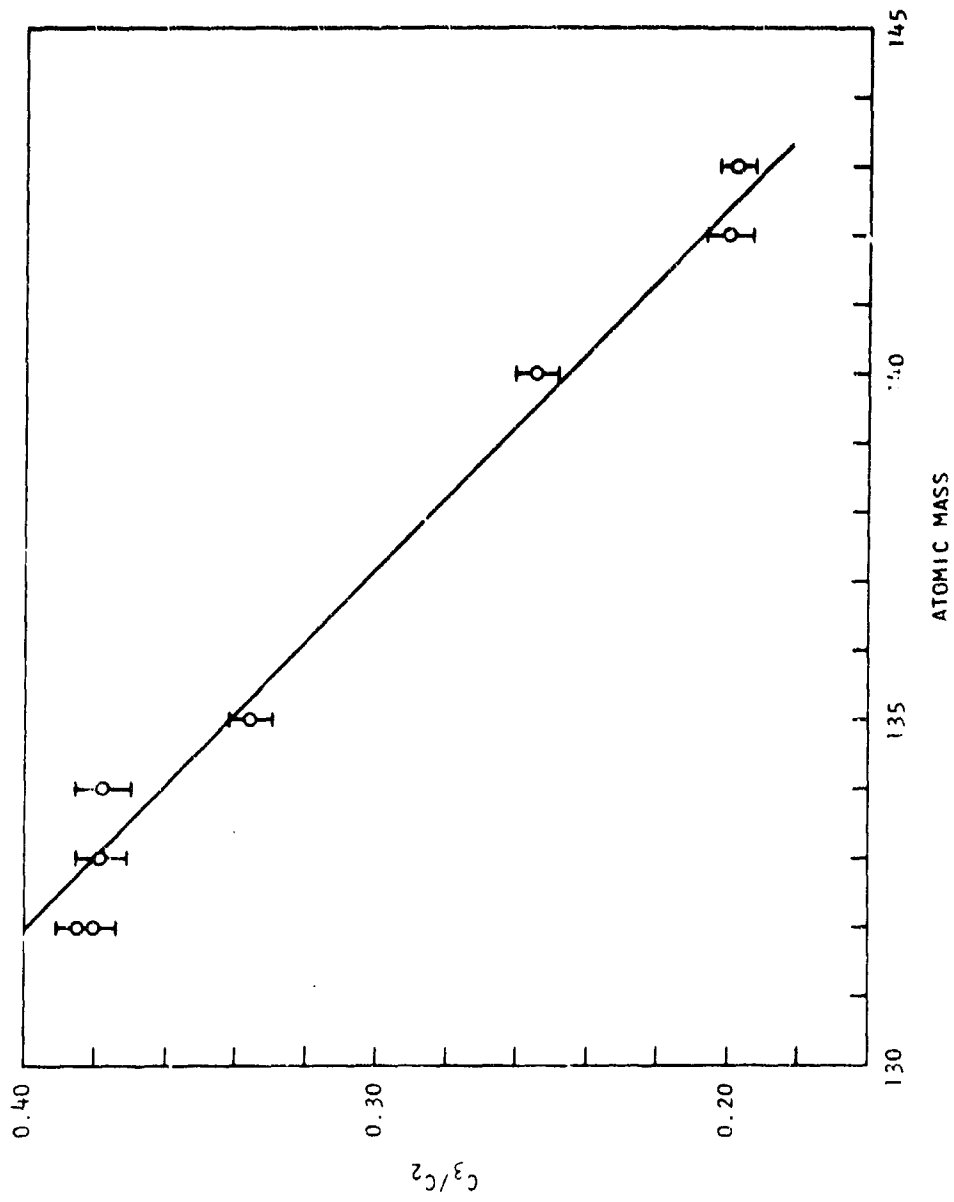


Fig. 3. Fission-product recoil-range parameter  $C_3/C_2$  in Mylar vs. atomic mass. Data taken from Ref. 1

were not particularly successful for obtaining the desired uranium density. A 1 to 2 micrometer thick foil of enriched uranium metal was quite expensive for the desired surface area. The source was prepared using a suggestion of Professor John W. Irvine, Jr., of M.I.T. A settling tower was fabricated from a 4-in.-diameter pyrex cylinder, open at both ends, that was weighted on top with a lead brick. The bottom of the tower was a piece of smoothed commercial aluminum foil separated from the cylinder by a silicon rubber O-ring. The aluminum foil had been covered with a thin film of dried shellac. The tower was partially filled with  $\text{CCl}_4$ , and the commercial uranium oxide powder (approximately 1 micrometer diameter fully enriched) was triturated with a drop of oil and then washed into a Waring blender using  $\text{CCl}_4$ . The mixture was blended and then poured into the tower. After settling overnight, most of the supernatant  $\text{CCl}_4$  was carefully drawn off and the remainder was evaporated. After the tower was disassembled, the uranium oxide film adhering to the foil was wetted with a shellac-ethanol mixture, dried, and heated to approximately  $100^\circ\text{C}$  in air for approximately 1 hr. This provided an adherent, reasonably uniform, thin preparation approximately  $7 \text{ mg/in.}^2$ . This preparation was approximately 2 to 3 micrometers thick with an equivalent roughness. It was cut into a selected 2-1/2 in. by 1-1/2 in. rectangle, covered with a 6-micrometer Mylar sheet, and taped to the concave surface of the source holder.

The tape system has capstan drive controls with a wide dynamic range, allowing tape speeds of 0.1 to 60 in./sec. For high speeds, a magnetic transducer on the capstan flywheel allows frequency measurements to be made using an ac amplifier and an electronic scaler. The frequency is converted to tape speed using calibration graphs to provide close control of delay times. Supply reels and take-up reels, operated by dc servo motors, maintain tension on the tapes during operation.

Gamma spectra, obtained with the 4096-channel analyzer, were read out onto IBM tape that was processed in the Univac 1108 computer. The code (GGAMPUTE) provides output from the two 2048 spectra in the form of gamma energies, background intensities, corrected integrated peak intensities (dpm), and counting statistics. A subroutine allows the unfolding of complex

unresolved spectra using as a model sums of Gaussian distributions with an exponential background function.

The main problem so far has been in obtaining sufficiently accurate data. For nuclide mass correlations, signal ratio accuracies of approximately 5% are needed. The apparatus does not seem to pose problems in this respect. A sufficiently close duplication of delay times and counting periods and a good calibration of detector sensitivities can be made so that recoil range parameters can be measured within 5%. Also, uniformity of the tapes should play only a minor role since only a comparison of "average ranges" is necessary. However, peak interference in the spectra is rather important since signal intensity accuracy is affected adversely by interfering peaks, and identification of fission products from recoil ranges is not definitive without precise intensity measurements. The accuracy of counting as a function of delay time may not require quite the precision that the range measurements do, but accuracy is important for this determination also.

Because peak intensity is such a limiting factor, plans have been made to place the source and part of the tape system at the bottom of the beam tube to greatly increase the fission rate. This will increase the neutron flux at least four orders of magnitude, with about three orders increase in gamma signals. Minimum delay times will be lengthened since the tape must travel ten times further from the source to the detector. In this configuration, the minimum delay time will be approximately 5 sec instead of 0.5 sec. However, the increase in signal intensity and the better time definition of the signal should more than compensate for the higher minimum delay time.

#### EXPERIMENTAL RESULTS

Thus far, two experiments have been performed to check the apparatus and method and to disclose major sources or problems. The preliminary studies were made in the low energy portion of the spectrum. The energy scale was established for both detectors using appropriate standards. Background spectra were obtained either with the source removed, the neutron

beam present and the tape moving, or with the tape stopped. No differences were noted. A 60-min experiment was done using a tape speed of 7.5 in./sec, corresponding to a delay time of 4.0 sec from source to detectors. The background-corrected spectrum exhibited a considerable number of peaks for the tape adjacent to the source, although few peaks were observed in the background-corrected spectrum for the second tape. The energies for prominent peaks from the first tape are listed in Table 1.

TABLE 1  
A LIST OF PROMINENT PEAKS IN SPECTRUM FROM TAPE ADJACENT TO SOURCE  
IN THE 60-MIN EXPERIMENT WITH DELAY TIME OF 4.0 SEC

keV	Assignment	keV	Assignment
96.12 <sup>(a)</sup>	(Nb-99)	178.36	
102.50 <sup>(a)</sup>	(Xe-140)	210.99 <sup>(a)</sup>	(Xe-140)
107.56 <sup>(a)</sup>		217.99 <sup>(a)</sup>	(Xe-139)
120.58	(Kr-90)	240.62	
128.98		257.91 <sup>(a)</sup>	
132.31		275.21 <sup>(a)</sup>	
136.31 <sup>(a)</sup>		294.82	(Xe-139)
145.01		331.72	
153.67		467.93	
157.35 <sup>(a)</sup>	(Ba-143)	504.46	
173.35 <sup>(a)</sup>		535.33 <sup>(a)</sup>	
		594.43	

<sup>(a)</sup> Most prominent.

There were several peaks that were not as well resolved in the spectrum below 96.12 keV; however, uncertainties in the energy calibration in that region did not warrant assignment of these energies.

In the second experiment, the tape speed was 1.3 in./sec, corresponding to a delay time of 23 sec. Three 80-min spectra were obtained, each preceded and followed by a 20-min background spectrum. The spectra were electronically added and corrected for background. Part of the resulting spectra for both

tapes are shown in Figs. 4 and 5. These spectra have an artificial background of 305 counts/channel in addition to an uncorrectable Compton background from the desired signal. The data were derived using 0.33 keV/channel. The data are summarized in Table 2.

TABLE 2  
PROMINENT PEAKS IN SPECTRA FROM TWO TAPES FOR THE 240-MIN EXPERIMENT  
WITH A DELAY TIME OF 23 SEC

E(keV) <sup>(a)</sup>	$\Delta E$ (keV) <sup>(b)</sup>	I (cpm) <sup>(c)</sup>	Ratio <sup>(d)</sup>	Nuclide <sup>(e)</sup>	$t_{1/2}$ (sec) <sup>(f)</sup>
93.65	0.29	10.4	$0.53 \pm 0.04$	Mo-105	58
97.65	0.15	18.9	$0.41 \pm 0.03$	Nb-99	10.5
103.79		12.6	<0.15	Xe-140	13
121.36	0.17	25.4	$0.55 \pm 0.02$	Kr-90	24
129.91		3.3			
137.45	-0.03	42.9	$0.39 \pm 0.01$		
156.12		12.2	<0.15	Ba-143	12.6
211.03		17.5	<0.10	Xe-140	13
218.38		24.5	<0.10	Xe-139	41
296.28		8.4	<0.20	Xe-139	41
344.50	0.28	4.7	0.45		
397.33		13.8	<0.15	La-144, Ba-144	41, 11
492.28		3.9	$0.45 \pm 0.07$		
540.07	1.15	8.4	$0.22 \pm 0.04$	Kr-90	24
602.86	-0.43	7.3	$0.15 \pm 0.05$	Cs-140	58

- (a) Energy from spectrum for the tape adjacent to the source.  
 (b) Energy differences for spectra from the two tapes.  
 (c) Integrated peak intensity for the tape adjacent to the source by GGAMPUTE.  
 (d) Intensity ratio for the two tapes.  
 (e) Tentative assignment.  
 (f) Corresponding to (e).

In Table 2, the intensity ratios clearly fall into two groups that are qualitatively correlated with nuclide mass: a high ratio (approximately

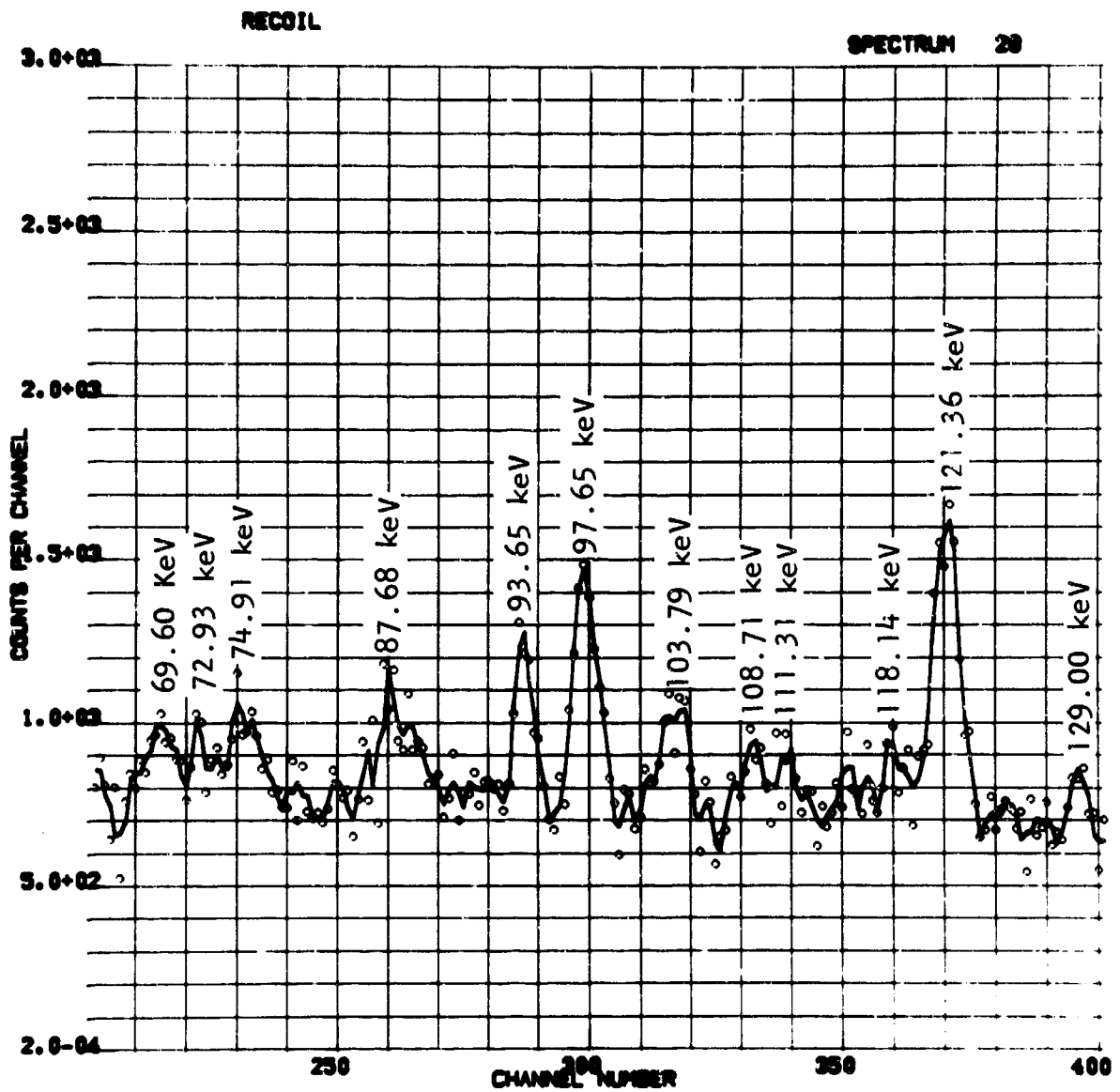


Fig. 4. Part of spectrum from the moving tape adjacent to the source.  
Curves are smoothed data (Sheet 1 of 2)

RECOIL

SPECTRUM 20

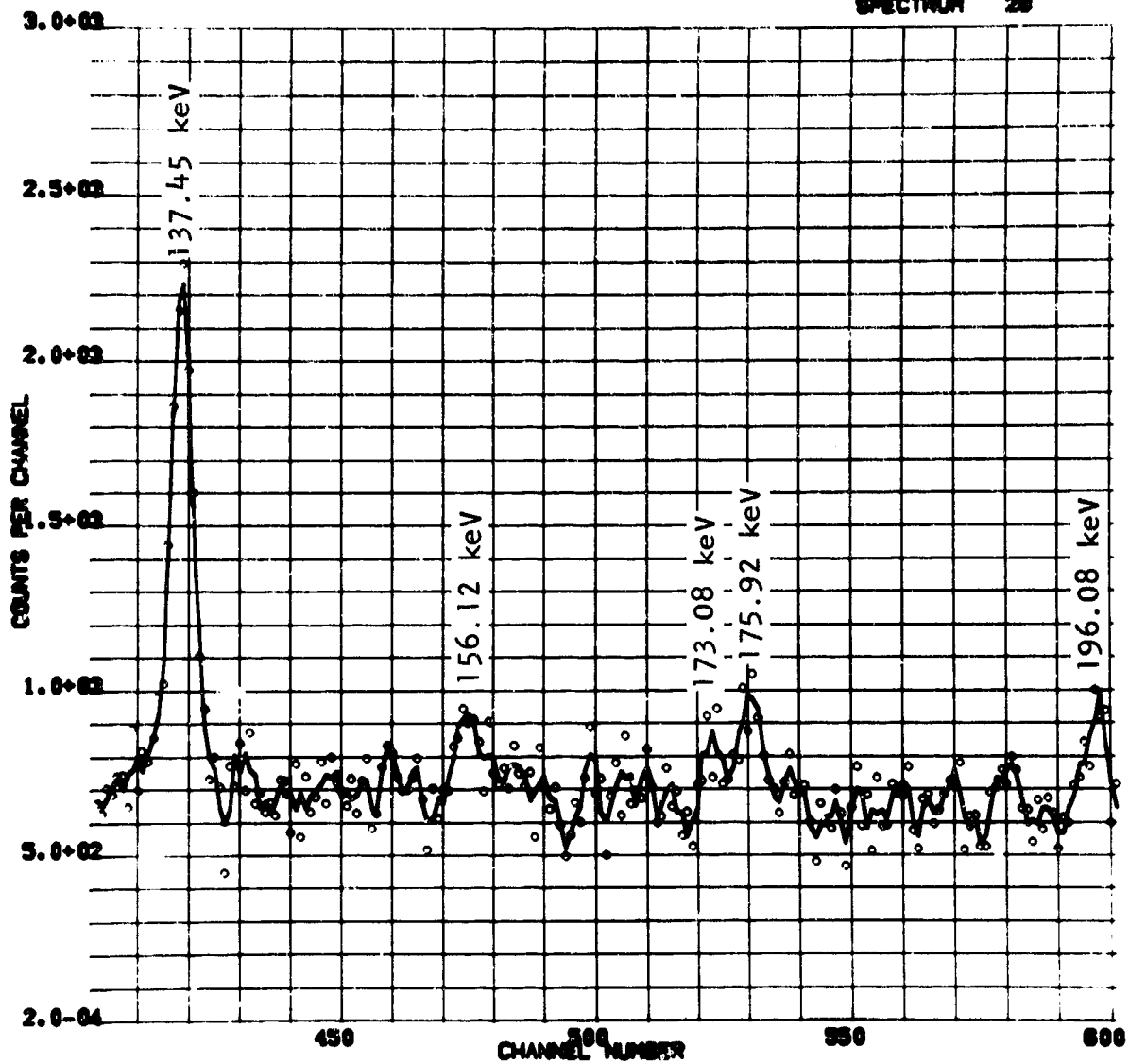


Fig. 4. Part of spectrum from the moving tape adjacent to the source.  
Curves are smoothed data (Sheet 2 of 2)

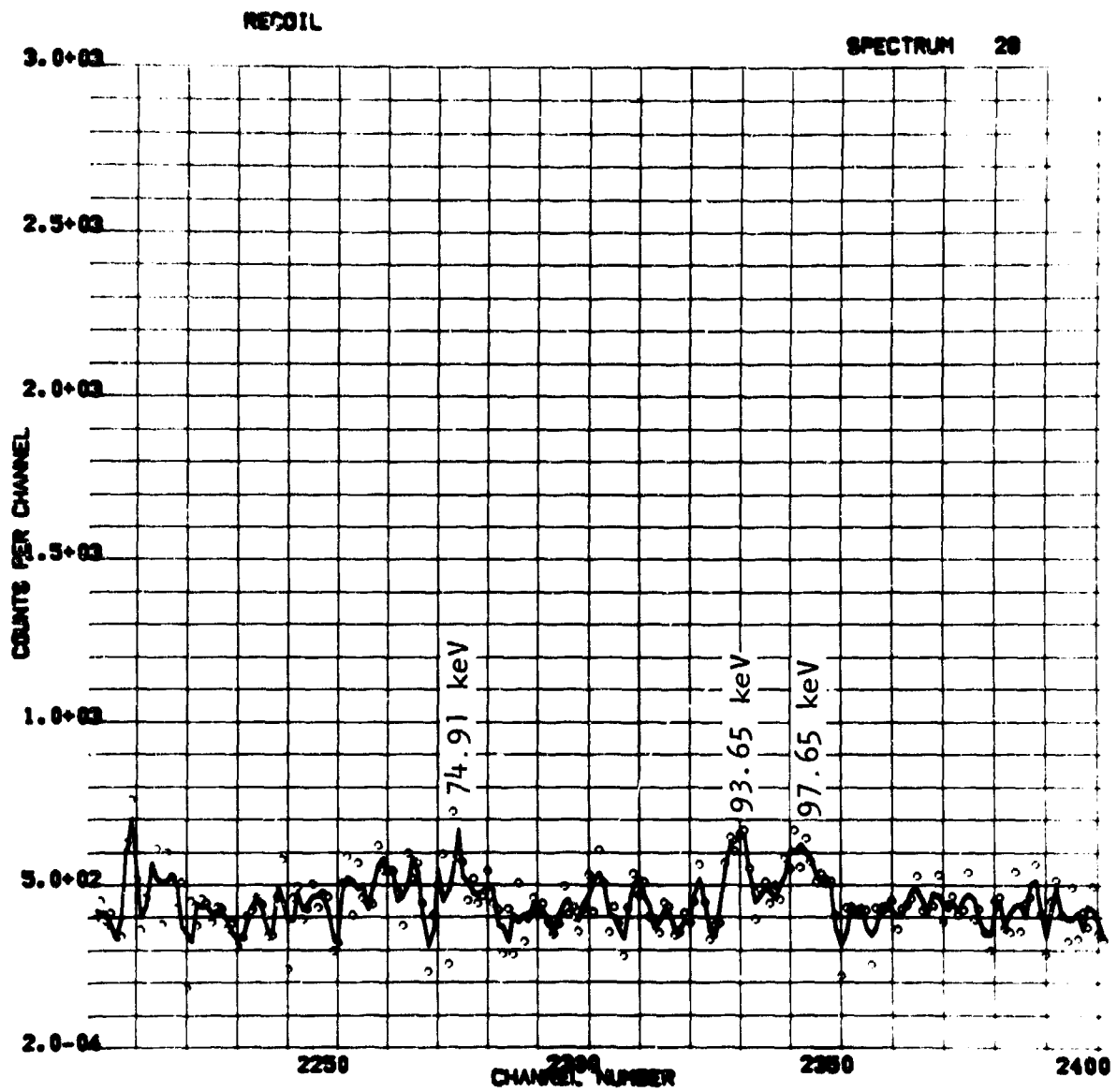


Fig. 5. Part of spectrum from the moving tape furthest from the source.  
Curves are smoothed data (Sheet 1 of 2)

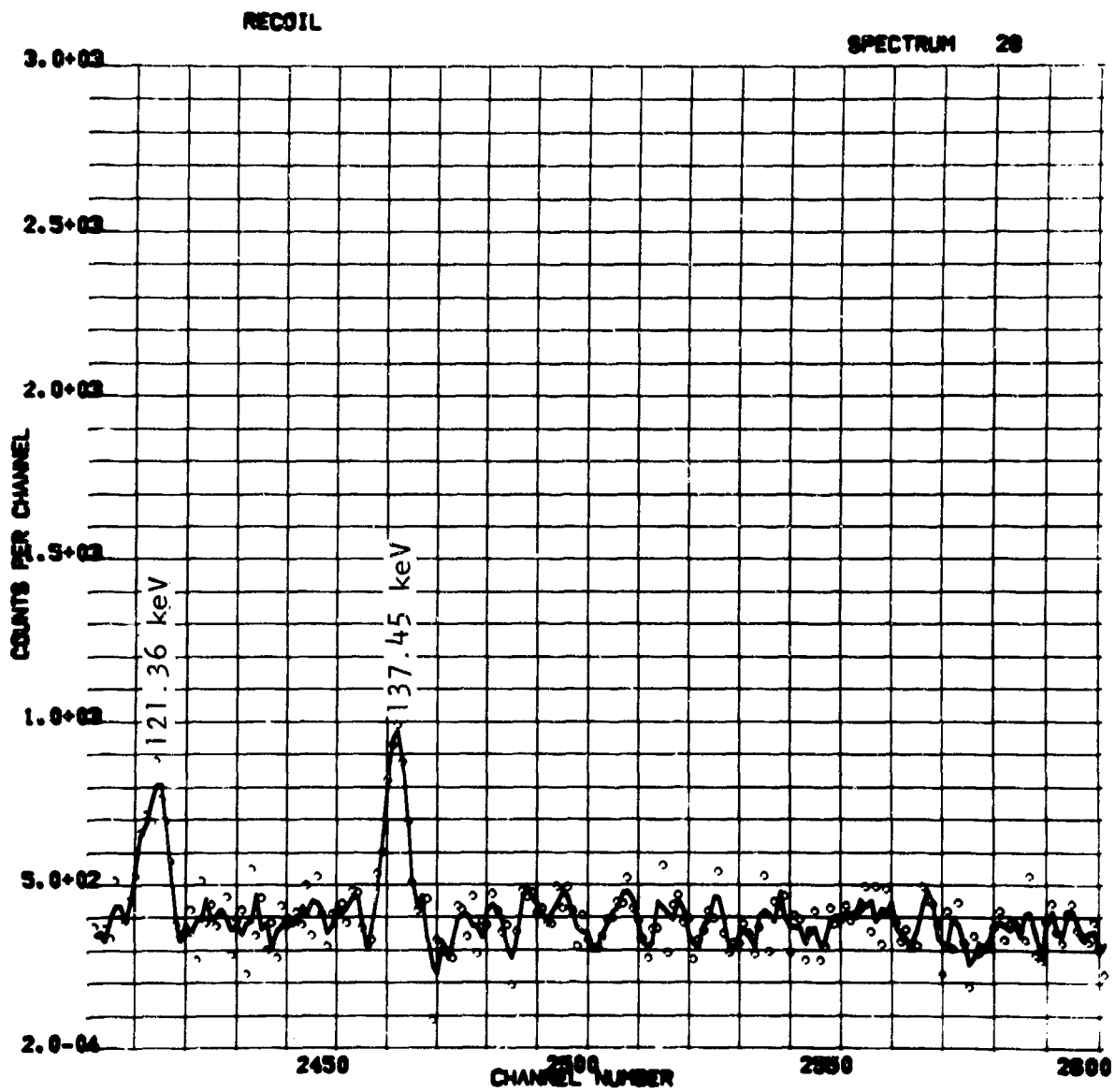


Fig. 5. Part of spectrum from the moving tape furthest from the source.  
Curves are smoothed data (Sheet 2 of 2)

0.5) indicating low mass, and a low ratio (less than 0.20) indicating high mass. Because of the small signals, it was impossible to obtain a quantitative correlation as that previously obtained for a static tape system (Ref. 1). The present data (with the possible exception of the 540 keV peak) indicate that the recoil range method should be capable of yielding the desired data if signal strength can be increased.

The data in Table 2 were obtained from the output of the Univac 1108 treatment of the raw data and from the channel-signal printout of the TMC analyzer. The spectra were then converted to digital tape and were plotted. Perusal of the plot for the tape adjacent to the source disclosed other peaks of lesser intensities, some of which had been ignored by the computer program. These peaks are listed in Table 3.

TABLE 3  
ADDITIONAL PEAKS FROM 240-MIN EXPERIMENT  
FOR TAPE ADJACENT TO SOURCE  
(Energies in keV)

64.78	118.14	381.19
69.60	173.08	388.00
72.93	175.92	455.20
74.91	196.99	466.84
87.68	257.95	511.03
108.71	288.89	543.23
111.31	292.49	594.97

It is emphasized that the assignments of nuclides to photopeaks in Tables 1 and 2 are speculative. The assignments are based upon the pioneering work of Alväger et al. (Ref. 3) and Wilhelmy (Ref. 4), both of whom used Cf-252 sources. However, the yield curves for spontaneous fission of Cf-252 and thermal neutron-induced fission of U-235 are very different, especially in the regions of the maxima. If the assignments in Tables 1 and 2 are correct, then there is excellent agreement between these energy values and those reported by Alväger et al and Wilhelmy. The standard deviation is approximately 0.35 keV, which corresponds to approximately 1 channel in 4096.

From Kochenderfer's (Ref. 5) computation for instantaneous thermal neutron fission of U-235, one might expect to observe photopeaks, in the time regime studied so far, that correspond to Kr-91, Rh-92, Rb-93, Zr-100, Na-143, La-144, and La-145 for example. However, gamma efficiencies, energies of the photopeaks, and yields, together with the half lives, all dictate the importance of these nuclides in the present study.

A small amount of data about half-life values could be derived from our two experiments. These data are only qualitative since birth-and-decay laws of families require at a minimum that one measure a decay rate of a particular species a number of times equal to the number of important precursors plus two. Thus, two measurements would suffice only if there were no important precursors. The data are in line with observing species whose half-lives range down to at most 3 or 4 sec in some cases.

The experiment reported in the last final report (Ref. 1) established the feasibility of the double-tape method for determining atomic masses by recoil ratios. The preliminary data reported herein confirm this. All of the required instrumentation and apparatus, with exception of the tape guide to the bottom of the neutron beam tube, are available for quantitative studies when time is available with the Gulf General Atomic Mark III TRIGA beam tube. No difficulties are foreseen in extending the source and tape system to the near vicinity of the thermal neutron column.

Since these are the first Ge-Li detector studies of many simultaneously borne short-lived fission products from thermal neutron irradiation of uranium reported, the work involves a correlation of half lives, atomic masses, and gamma energies that are not well characterized, if at all. The quantitative description of nuclides according to half lives,  $(N, t_{1/2})$ , will require establishing the  $N-t_{1/2}$  scale carefully for intermediate values of  $t_{1/2}$  and then successively extending the studies to shorter values of  $t_{1/2}$ .

We conclude that the system and approach have been proved. The future quantitative experiments should be most fruitful.

## FISSION PRODUCT SORPTION RATE MECHANISMS

In last year's final report (Ref. 1), a discussion of the role of condensed-state diffusion coefficients and condensation coefficients as applied to fallout formation was presented. This discussion was based on a description of surface-limited sorption presented by Crank (Ref. 6). Basically, if no gas-phase diffusion problem exists and  $\alpha = \alpha_t = \alpha_e$  (the evaporation coefficient equals the condensation coefficient, and these values are independent of concentration), then

$$F = 1 - \sum_{n=1}^{\infty} \frac{6(rh)^2}{\beta_n^2 [\beta_n^2 + rh(rh-1)]} \exp\left(-\frac{\beta_n^2 Dt}{r^2}\right), \quad (1)$$

where  $\beta_n \cot \beta_n = 1-rh$ . In this expression  $F$  is the fractional sorption at time  $t$  (sec), starting with an initially unloaded particle of radius  $r$  (cm), in an atmosphere where the sorbing substance is at a constant pressure. The value of  $h$  is given by the expression

$$h = \frac{44.33H\alpha}{D\rho} \left(\frac{M}{T}\right)^{\frac{1}{2}}, \quad (2)$$

where  $H$  is the Henry's law constant [atm/(g/g)],  $M$  is the gaseous species molecular weight (g/mole),  $T$  is the temperature ( $^{\circ}$ K),  $D$  is the diffusion coefficient ( $\text{cm}^2/\text{sec}$ ), and  $\rho$  is the matrix density ( $\text{g}/\text{cm}^3$ ). In our report (Ref. 1) we expressed the opinion that for systems where  $rh$  is greater than 10, one can consider the system to be condensed-state-diffusion controlled. This opinion was expressed on the basis of the figure in Ref. 6 describing  $F$  as a function of  $(Dt/r^2)^{1/2}$  for a series of  $rh$  values. While this is a reasonable description according to this figure, it is apparent that  $F$  values at very low  $Dt/r^2$  values should be further considered since  $rh$  values that

lead to small F values can be quite important in describing the sorption of highly fractionated elements during fallout formation. The region of small F values essentially requires computer techniques to obtain solutions to Eq. 1 because of the problem of obtaining  $\beta_n$  values and making the necessary summations using these terms. In our calculations, an n up to 30 with  $\beta_n$  accuracies of 8 decimals was necessary to arrive at accurate F values. Calculations have been made for  $rh = \infty$  and  $rh = 1$  where accurate  $\beta_n$  values are not difficult to obtain (i.e.,  $\cot \beta_n = \infty$  and 0, respectively).

One can describe the results of the calculations in terms of two limiting differentials. The first differential is

$$\lim_{Dt/r^2 \rightarrow 0} \left[ \frac{Dt/r^2}{F} \frac{dF}{d(Dt/r^2)} \right] = \lim_{Dt/r^2 \rightarrow 0} \left[ \frac{d \ln F}{d \ln(Dt/r^2)} \right] = 1 \quad (3)$$

for any value of rh less than  $\infty$ . That is,

$$F = At, \quad (4)$$

where A is a constant, will describe Eq. 1 at sufficiently low values of  $Dt/r^2$ . This result is consistent with a condensation-rate-controlled process at sufficiently short times and confirms the form of this expression for short times. The second differential is

$$\lim_{Dt/r^2 \rightarrow 0} \left[ \frac{dF}{d(Dt/r^2)} \right] = \sum_{n=1}^{\infty} \frac{6(rh)^2}{\left[ \beta_n^2 + rh(rh-1) \right]} \quad (5)$$

Thus, the expression for F as  $Dt/r^2 \rightarrow 0$  becomes

$$F = \frac{6Dt}{r^2} \sum_{n=1}^{\infty} \frac{1}{\left[ (\beta_n/rh)^2 + 1 - 1/rh \right]} \quad (6)$$

which establishes the  $rh$  spacing between sorption curves. The summation approaches  $rh/2$  and thus

$$F \rightarrow \frac{132.99 H\alpha}{r\rho} t(M/T)^{\frac{1}{2}}, \quad (7)$$

which is precisely a description of a condensation-rate-limited process.

From these results, Fig. 6 was constructed, which presents curves for  $F$  versus  $(Dt/r^2)^{1/2}$  at a series of  $rh$  values. The circled points are the only calculated points; thus, the limiting lines shown for  $rh$  values other than 1 and  $\infty$  were obtained by synthesizing curves from the limiting behaviors. The family of curves helps in understanding fallout fractionation processes.

In Fig. 6, the calculated points for  $rh = 1$  are in agreement with the system exhibiting condensation-rate-limited sorption. For other values of  $rh$  less than one the behavior will be similar. For  $rh$  greater than one the opportunity exists for the  $F$  value to approach the  $F$  value for condensed-state diffusion control (the  $rh = \infty$  curve). When this happens the sorption controlling process changes over from a condensation-controlled process to a condensed-state diffusion-controlled process. Of course, an  $F$  region exists where the two rate processes are competitive.

The important questions concerning fallout formation (temporarily excluding dominance of gas diffusion) are the appropriate values of  $rh$  and  $F$ . One must deal with two fractionation processes. With respect to fallout particles, an element becomes supersaturated in the nuclear cloud because (1) the cloud is cooling or (2) the volatile parent of the condensing fission product is decaying. These two processes generally occur in different regions of  $rh$  and  $F$  values of Fig. 6.

In the first case, one can assign  $H$ ,  $\alpha$ ,  $D$ ,  $r$ , and  $F$  values to the process to determine the controlling phenomenon. During the sorption of the majority of a particular species from a nuclear cloud, the values of  $F$  are

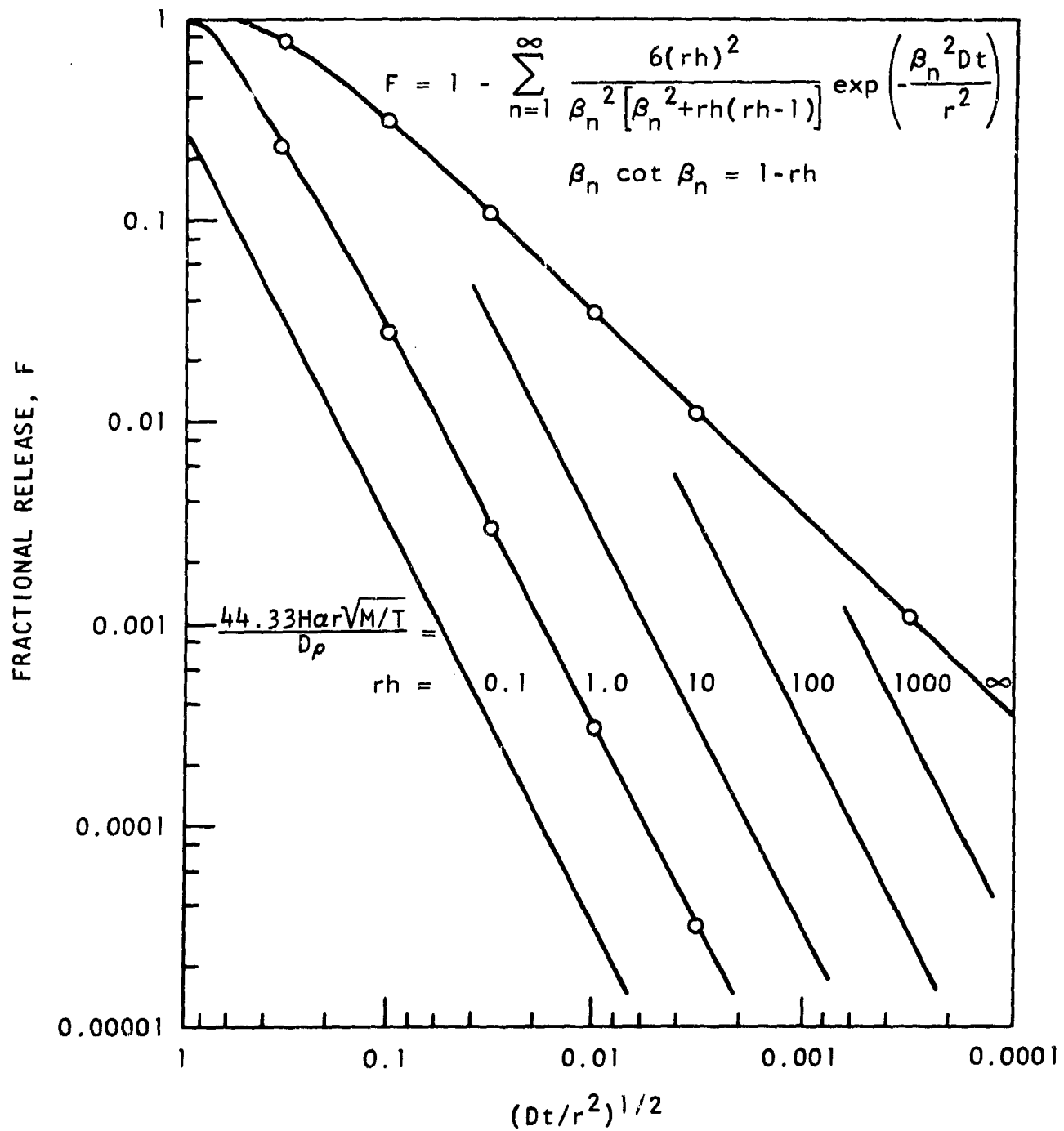


Fig. 6. Fractional sorptions as a function of time for varying values of  $rh$

not particularly small for important cases; H values are approximately 1 and thus, for the various size particles, an estimate of whether  $\alpha$  or D is the important property can be made using Fig. 6 and the appropriate data.

In the second case, H and F often become very small, which can drive the process into a condensation process or gas-phase diffusion process or both. (Of course, D may also become very small.)

The foregoing considerations can now be extended to include the considerations of gas-phase diffusion limitations. Freiling (Ref. 7), has suggested a solution to this question in terms of resistivities to transport and proposes the term "degree of control" as given by a fraction of the total resistivity associated with a particular phenomenon. Freiling's approach appears worthwhile, but application of it is more complex than he indicates. Comparing normalized rates of the individual processes under the appropriate conditions is the proper approach, but the simplified formulae for rates that he presents are appropriate only for specific conditions. The rates of the three important processes do not scale in the same way with loading; thus, more complex parameters must be considered. An extension of the analysis to include the scaling problem with loading should therefore be developed.

As a partial solution to this problem, Fig. 7 is presented to describe the rates of these processes for the condition of exposure to an isothermal nondepleting atmosphere in the form of varying values of  $\alpha/D_c$  and a single selected value of  $D_v$ , where  $\alpha$ ,  $D_c$ , and  $D_v$  are the condensation coefficient, the condensed-phase diffusion coefficient, and the vapor-phase diffusion coefficient, respectively. The other terms presented in this figure have been defined previously. The selected  $D_v$  value defines a sorption curve that has the same time dependence as a condensation-controlled curve. It serves as a limiting curve; that is, material cannot be sorbed at a greater rate than gas-phase diffusion will allow. Thus, in Fig. 7 no fractional sorption to the right of the selected  $D_v$  curve exists. This is shown by crosshatching the region to the right of the  $D_v$  curve. The condensed-state diffusion limitation can be stated similarly: no fractional sorptions to the right

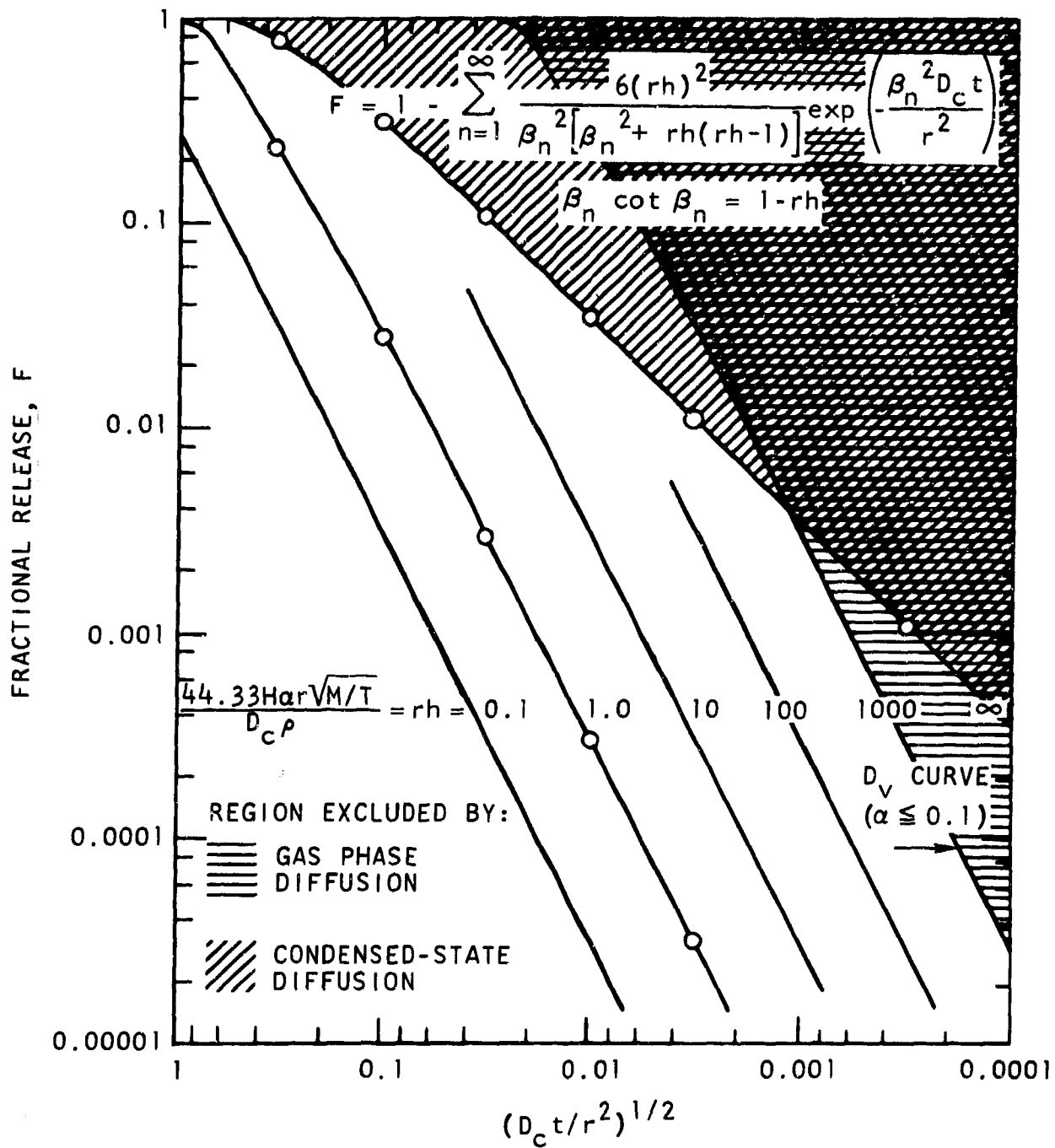


Fig. 7. Fractional sorptions as a function of time for varying values of  $rh$ , showing regions of gas-phase diffusion and condensed-state diffusion control

of the condensed-state diffusion curve exist. This region is also cross-hatched. Thus, if condensation coefficients are sufficiently large ( $\geq 0.1$ ), the sorption process will be governed by the gaseous diffusion until it encounters (if this happens at all) the condensed-state diffusion control. The reason for selecting  $\geq 0.1$  as a limit is that the meanings of  $\alpha = 1$  and condensation coefficient control require that every molecule of the condensing species that strikes the fallout particle condenses and that none of these molecules re-evaporate. This describes exactly a condition that must be limited by diffusion in the gas phase since a large concentration gradient in the gas phase must exist. We have assumed that gas phase diffusion control will extend to somewhat lower  $\alpha$  values than unity. The actual sorption process depends on the intersection of the gas-phase-diffusion or condensation-coefficient controlled curve (one or the other only) with the condensed-state-diffusion controlled curve.

## EXPERIMENTAL CONDENSATION COEFFICIENT STUDIES

Concomitant with the theoretical studies of the importance of condensation coefficients in the fallout problem reported previously (Ref. 1) and reported here, an experimental program was initiated at the Gulf General Atomic, atomic beam facility.

A first experimental consideration of the importance of condensation coefficients, flat samples of  $\text{CaO-Al}_2\text{O}_3\text{-SiO}_2$  eutectic glass, formed at approximately 1700°K and heated to 700°K in a vacuum for the experiment, were exposed to helium and argon beams directed 50 deg from the normal to the glass surface. The 1200°K argon beam was scattered essentially according to the cosine law. Room temperature helium and 1600°K helium were scattered similarly, exhibiting near-cosine scattering. There were no indications of specular scattering.

In an ideal case a species with a low condensation coefficient should be scattered specularly from a flat, clean surface. It was hoped that the glass would present a flat, clean surface to the beam, but the supposed non-condensing beams of argon and helium were shown not to reflect specularly. Thus, there appears to be little hope that metal oxide beams could show specular reflection from these surfaces. Cleaning of the glass surfaces by heating to higher temperatures might lead to specular reflections of argon and helium. However, to do this the glass should be heated to at least 1500°F in the apparatus, which is difficult experimentally at this time.

In the problem of fallout formation, it is difficult to characterize a fallout particle surface sufficiently well to be able to predict fission product behavior during fallout formation if this behavior is governed by condensation coefficients.

## DIFFUSION OF RADIOACTIVE NUCLIDES IN MOLTEN SILICATES

In the last final report (Ref. 1) diffusion coefficients were predicted for the transport of cesium in a molten medium of albite composition;  $\text{Na}_2\text{O}-\text{Al}_2\text{O}_3-6\text{SiO}_2$ . A study of this system has been completed. Diffusion experiments were performed in the temperature range 1417 to 1669°K using the plane source technique which has been previously described in detail (Ref. 8). Sources were prepared by introducing high-specific activity Cs-134 into the glass at about the 0.01% level. Sectioned samples were monitored by observing the 0.60 MeV photopeak using a 0.10 MeV window. All of the data were treated using the method of least squares. The data are summarized in Eq. 8, Fig. 8, and Table 4.

$$\log_{10} D = 0.22 - (8.62 \times 10^3/T) \quad (8)$$

TABLE 4  
DIFFUSION COEFFICIENTS FOR TRANSPORT OF RADIOCESIUM  
IN MOLTEN MEDIA OF ALBITE COMPOSITION

T (°K) (a)	D (cm <sup>2</sup> /sec) x 10 <sup>6</sup> (b)
1417	1.1
1417	1.4
1504	3.0
1510	3.1
1589	8.1
1669	9.9
1669	10

(a)  $\pm 10^\circ\text{K}$ .

(b)  $\pm 18\%$ .

The predicted diffusion coefficients for this system (Ref. 1) were described by the equation:

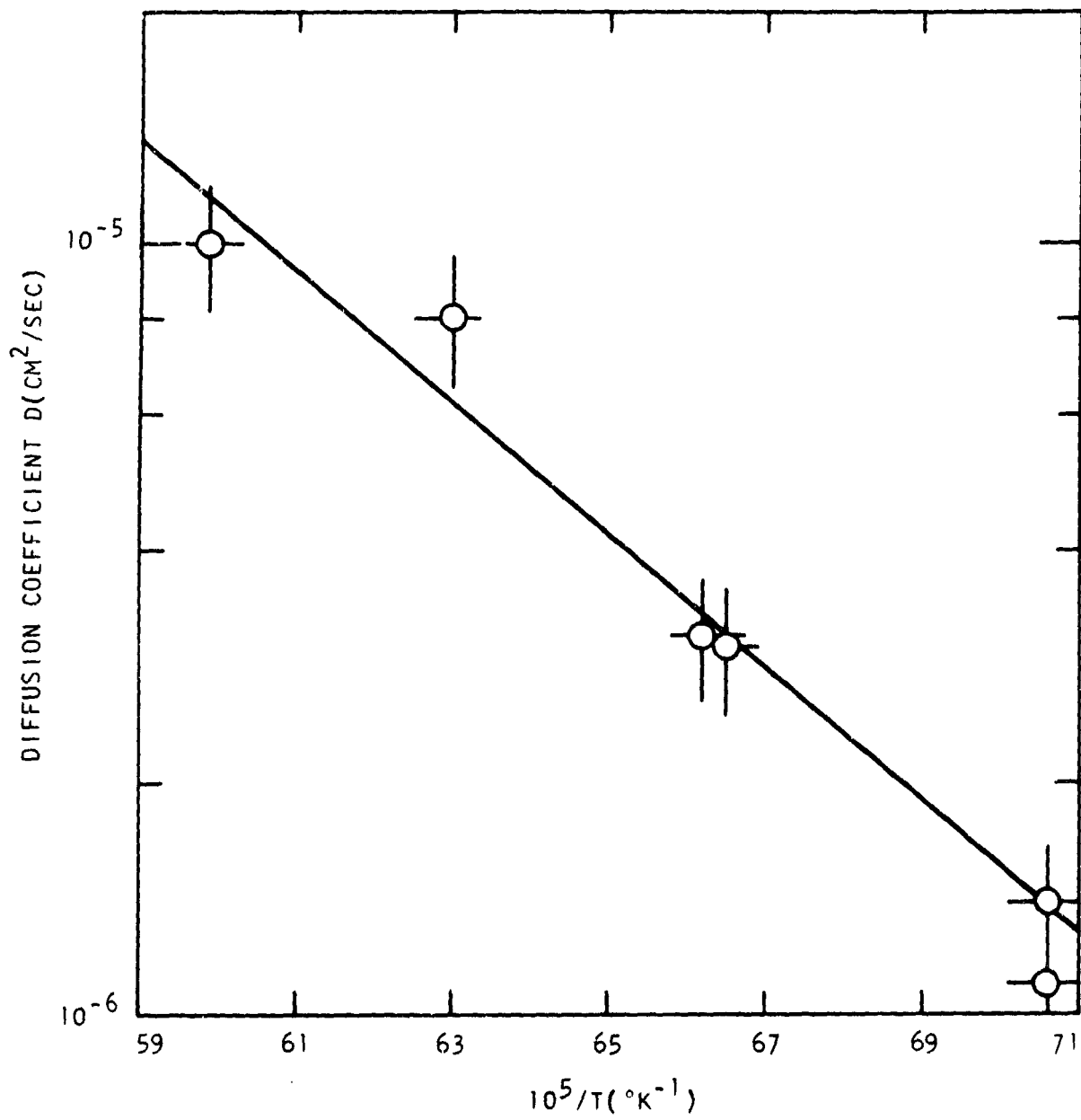


Fig. 8. Diffusion coefficients for transport of radiocesium in molten media of albite composition as a function of temperature

$$\log_{10} D = 0.17 - (8.00 \times 10^3/T) . \quad (9)$$

There is good agreement between the coefficients in Eq. 8 and those in Eq. 9, the differences falling within experimental error. This experiment again demonstrates good reliability of predicted diffusion coefficients.

Using Eq. 8 together with previously reported data for transport of sodium in molten media of albite composition (Ref. 1), it is possible to make a more reliable prediction of the behavior of I, Rb, K, and Li in the same medium than was possible in the last final report (Ref. 1). This has been done by assuming that compensation prevails (Ref. 9),

$$\log_{10} D_0 = a + bE^* , \quad (10)$$

and that  $E^*$  is a linear function of the reciprocal ionic radius (Ref. 8):

$$E^* = m + nr^{-1} . \quad (11)$$

In Eqs. 10 and 11,  $D_0$  is the pre-exponential factor and  $E^*$  is the activation energy in the Arrhenius equation. The results of this calculation are presented in Table 5.

TABLE 5  
ARRHENIUS PARAMETERS FOR DIFFUSION IN MELTS OF ALBITE COMPOSITION

Species	$E^*$ (kcal/mole)	$\log_{10} D_0$ ( $D_0$ in $\text{cm}^2/\text{sec}$ )	Remark
I	41.4	0.38	predicted
Cs	39.4	0.22	experimental
Rb	38.1	0.11	predicted
K	36.9	0.01	predicted
Na	32.3	-0.36	experimental
Li	22.8	-1.14	predicted

The inclusion of iodine in the prediction is based upon previously obtained experimental evidence (Ref. 8).

Another study involved the self-diffusion of Na-26 in a glass that was purchased from the National Bureau of Standards. The glass, Standard Sample No. 710, has a composition of 70.5% SiO<sub>2</sub>, 8.7% Na<sub>2</sub>O, 7.7% K<sub>2</sub>O, 11.6% CaO, and 1.1% Sb<sub>2</sub>O<sub>3</sub>, and the viscosity as a function of the temperature is well-characterized.

Using the plane source technique (Ref. 8), experiments were performed in the temperature range 1041 to 1742°K. Sources were prepared from the same glass by irradiation in a Gulf General Atomic TRIGA reactor. Following irradiation, the sources were decayed for approximately 30 hr prior to use. The 1.37 MeV gamma peak was measured during sectioning using an 0.1 MeV total window. The data are summarized in Table 6 and are shown in Fig. 9.

TABLE 6  
DIFFUSION COEFFICIENTS FOR TRANSPORT OF  
Na-24 IN NBS-710 GLASS

T(°K) (a)	D(cm <sup>2</sup> /sec) × 10 <sup>7</sup> (b)
1742	190
1648	110
1422	45
1374	33
1225	11
1099	3.5
1041	1.8

(a) ± 10°K.

(b) Maximum uncertainty of 18%.

The data are also summarized in Eq. 12:

$$D = 1.70 \times 10^{-2} \exp\left(-\frac{2.35 \times 10^4}{RT}\right). \quad (12)$$

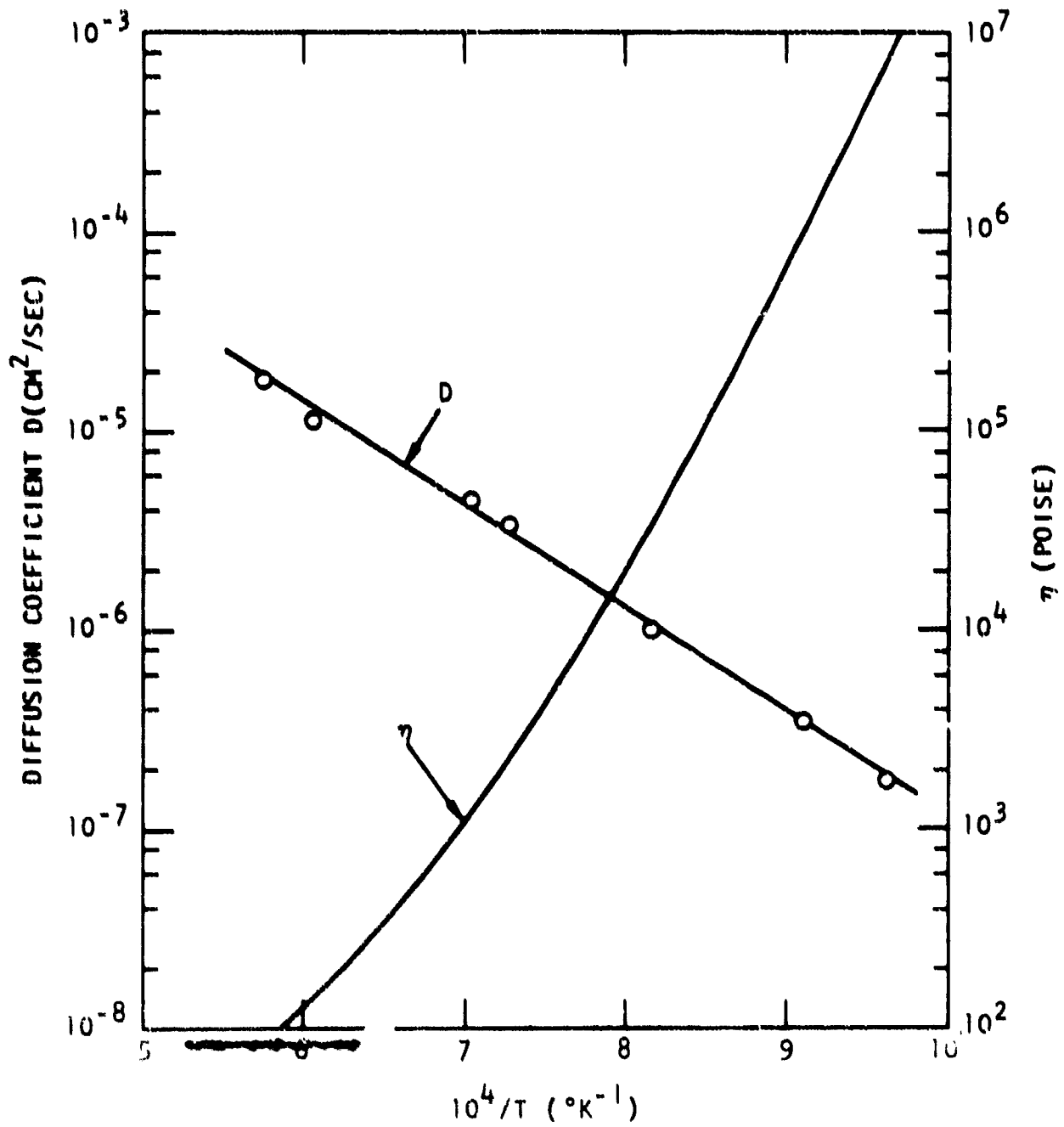


Fig. 9. Self-diffusion coefficient of Na-24 and viscosity as functions of temperature for NBS Standard Glass No. 710

The coefficients in Eq. 12 were obtained by the method of least squares. In Fig. 9, the line passing through the points is the least squares line. The viscosity data for this matrix are also shown in this figure.

Part of the purpose of this experiment was to obtain diffusion data of sufficient quality and over a sufficiently wide temperature range so that the applicability of the Stokes-Einstein equation to silicates could be quantitatively disproved. The Stokes-Einstein equation relates the diffusion coefficient and radius of the diffusing species with the viscosity of the medium,

$$D_r = \frac{kT}{6\pi\eta} \quad , \quad (13)$$

where  $k$  is the Boltzmann constant and  $T$  is the absolute temperature. Some authors have attempted to use this equation for metals, salts, and silicates (Refs. 10 and 11), and others have pointed out its inapplicability to silicates (Refs. 8, 12, and 13), although the statements concerning its inapplicability were only of a qualitative nature.

Using Eq. 13 with the experimental values for the diffusion coefficients and viscosities, species radii were calculated at several temperatures. (See Table 7.)

TABLE 7  
RADI AT VARIOUS TEMPERATURES USING EQUATION (13) AND  
EXPERIMENTAL DIFFUSIVITY AND VISCOSITY DATA

T(°K)	r(Å)
1707	$7.5 \times 10^{-4}$
1455	$2.1 \times 10^{-4}$
1292	$5.3 \times 10^{-5}$
1178	$1.2 \times 10^{-5}$
1095	$2.3 \times 10^{-6}$
1030	$4.3 \times 10^{-7}$

Since the ionic radius of sodium is  $0.95 \text{ \AA}$  (only slightly dependent on  $T$ ), and sodium is known to diffuse in silicates as  $\text{Na}^+$ , the data in Table 7 clearly show the error that may be encountered in indiscriminately using Eq. 13 for silicates. The calculated ionic radius changes by three orders of magnitude over a temperature interval of  $677^\circ\text{K}$ , which is clearly impossible. This result is not surprising since the Stokes-Einstein equation was derived for a large, uncharged particle moving through a medium of small uncharged particles, which is a poor model of transport of an ion in a molten silicate.

Studies of the diffusion of radionuclides in the  $1450^\circ\text{K}$   $\text{CaO-Al}_2\text{O}_3\text{-SiO}_2$  eutectic have continued. Considerable effort was made in testing a new approach to source-loading in the plane source technique (Ref. 8). Platinum capillaries were completely filled with molten  $\text{CaO-Al}_2\text{O}_3\text{-SiO}_2$  matrices in such a way as to provide a flat glass surface at the mouth of each capillary. A small piece of enriched uranium foil was fixed adjacent to the glass surface. After irradiation with neutrons in a Gulf General Atomic TRIGA reactor, thus recoil loading the glass, the uranium foil was removed and the samples were annealed at various temperatures. Following the anneal, the platinum was removed from the glass cylinders, using a molten lead bath, and the glasses were sectioned as previously described (Ref. 8). Using the 4096-channel, Ge-Li gamma detector system (Ref. 1), it was possible to obtain diffusion profiles at several temperatures for Xe, Nd, Ce, La, Te, Ba, Zr, Mo, I, and Nb.

The results of this study, in the temperature range  $1513$  to  $1823^\circ\text{K}$ , indicate small differences in the diffusion coefficients. At the highest temperature, diffusion coefficients ranged from  $5 \times 10^{-7} \text{ cm}^2/\text{sec}$  to  $8 \times 10^{-7} \text{ cm}^2/\text{sec}$ . At the lowest temperature, the range was  $2 \times 10^{-9} \text{ cm}^2/\text{sec}$  to  $1 \times 10^{-8} \text{ cm}^2/\text{sec}$ .

Perhaps the rate-limiting mechanism for the transport of the various radionuclides in the glasses was the diffusion of another species, for example, oxygen. However, one would expect that the recoiled radionuclides would have established their thermodynamically stable oxidation states with reference to air in the silicates in a very short period since the recoil ranges are of the order of only 10 micrometers.

In an attempt to clarify this problem, an experiment was performed with the simultaneous diffusion of Ce-144, Sr-85, Cs-137, and Co-60 in the reference eutectic glass at 1601°K using the plane source technique. Because of the low sensitivity of the Ge-Li detectors employed for the gamma analyses during sectioning, it was necessary to use a highly loaded source, approximately 30%. Thus, the matrix is not exactly comparable to that in which recoiled sources were used. The results of the experiment are shown in Fig. 10 where the logarithms of the concentrations, normalized with respect to Cs-137, are plotted against the square of the penetration distance. The curved lines in this figure may result from concentration-dependent diffusion coefficients in the region of the high loadings used. However, it is observed that the profiles for the four nuclides differ to the degree expected from previous diffusion studies not using recoil loaded sources. The problem associated with the recoiled sources has not been determined.

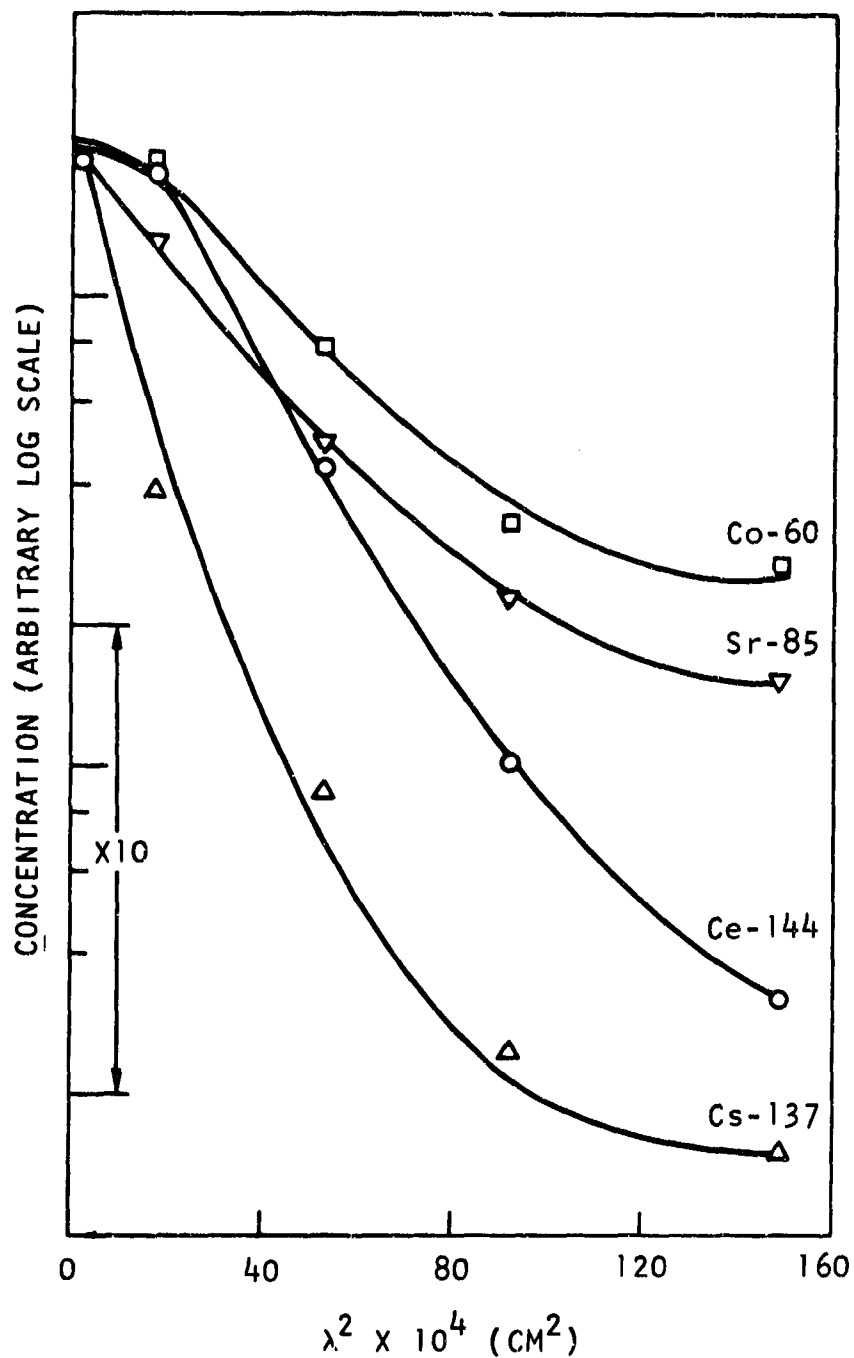


Fig. 10. Concentration profiles for simultaneous diffusion of radionuclides in 1450°K CaO-Al<sub>2</sub>O<sub>3</sub>-SiO<sub>2</sub> eutectic at 1601°K

## THERMODYNAMICS OF FISSION PRODUCT OXIDE SYSTEMS BY MASS SPECTROMETRY

Fission product oxide thermodynamic studies have been made on the fall-out program for the last few years. One of the fission products for which insufficient data are available is arsenic. We have been attempting to determine the stabilities of the oxides of this element using the mass-spectrometric Knudsen-cell method.

Calculations have been made to help understand the stability of AsO(g). Brewer (Ref. 14) reports energies of dissociation for As<sub>4</sub>O<sub>6</sub>(g) and AsO(g) of  $864 \pm 20$  kcal/mole and  $1.14 \pm 3$  kcal/mole, respectively. We have reported (Ref. 1) a value of  $309 \pm 4$  kcal/mole for the reaction



Combining these values with 120 kcal/mole for the reaction



yields 109 kcal/mole for the reaction



Measurements of the AsO(g) stability at 900°K were attempted. There was no difficulty in finding an AsO(g) signal, but there was a problem in finding an As<sub>n</sub>(g) signal and an O<sub>2</sub> signal concurrently with the AsO(g) signal.

A further attempt to observe an As<sub>n</sub>(g) species in equilibrium with O<sub>2</sub> and AsO(g) also failed. A 50-50 wt-% BaO-B<sub>2</sub>O<sub>3</sub> melt enabled extension of the

temperature range to 1300°C, but measurement of the three species in equilibrium was not feasible.

Estimates of the pressures for  $\text{As}_2(\text{g})$  and  $\text{O}_2$  were made at 900°K (assuming they were just below the mass spectrometric detection level) for the systems tried. An  $\text{AsO}(\text{g})$  pressure was measured and the  $\Delta S$  of formation was assumed to be the same as that found for  $\text{SbO}(\text{g})$  (Ref. 1). A minimum  $\Delta H = 108$  kcal/mole for the reaction in Eq. 16 was then calculated.

The  $\text{Sn-O}_2$  and  $\text{Ge-O}_2$  systems were investigated with the intent of measuring the stability of any  $\text{MO}_2(\text{g})$  species. The  $\text{SnO}_2(\text{s})$  was put into an Ir Knudsen cell. At temperatures up to 1400°C,  $\text{SnO}^+$  and  $\text{O}_2^+$  were the only parent ions detected. An appearance potential of  $10.1 \pm 0.5$  eV was measured for  $\text{SnO}^+$ . At 1330°C, with pressures of  $9.62 \times 10^{-5}$  atm and  $2.17 \times 10^{-4}$  atm of  $\text{O}_2$  and  $\text{SnO}(\text{g})$ , respectively, up to the detection limit for  $\text{SnO}_2(\text{g})$  (estimated as  $4 \times 10^{-9}$  atm), no signal was noted.

A  $\text{GeO}_2$  powder, which became glassy during the experiments, was used as the starting material in the study of the  $\text{Ge-O}_2$  system. The parent ions,  $\text{O}_2^+$  and  $\text{GeO}^+$ , and a previously unreported  $\text{GeO}_2^+$  were detected. Appearance potentials of  $11.3 \pm 0.5$  eV, and  $11.6 \pm 0.5$  eV were measured for  $\text{GeO}^+$  and  $\text{GeO}_2^+$ , respectively. The value for  $\text{GeO}^+$  is in good agreement with  $11.5 \pm 0.5$  eV recently reported by Hildenbrand (Ref. 15). The  $\text{GeO}_2^+$  fragment was not observed when the solid phase conditions were changed so that  $\text{Ge}_2\text{O}_2(\text{g})$  and  $\text{Ge}_3\text{O}_3(\text{g})$  were present.

An isothermal oxygen-dependence study showed that the equilibrium



could be studied. Temperature dependence studies yielded values for  $\Delta H_T^\circ$  of 43.4, 39.0, 39.5, 39.2, 35.6, and 39.1 kcal/mole, with the average value being  $39.3 \pm 2.8$  kcal/mole. The approximate midtemperatures of the study was 1540°k.

Two pressure calibrations were made by comparing a  $\text{Ag}^+$  signal with the other species. These results, with the calculated  $\Delta S_T^\circ$  for the reaction in Eq. 17, are listed in Table 8.

TABLE 8  
RESULTS OF PRESSURE CALIBRATIONS AND  
 $\Delta S_T^\circ$  CALCULATIONS FOR REACTION (EQ. 17)

Cal. No.	Temp	$P_{\text{O}_2}$ (atm)	$P_{\text{GeO}}$ (atm)	$P_{\text{GeO}_2}$ (atm)	$\Delta S_T^\circ$ (eu)
1	1536	$2.05 \times 10^{-5}$	$6.72 \times 10^{-5}$	$7.52 \times 10^{-9}$	33.0
2	1571	$4.09 \times 10^{-5}$	$1.52 \times 10^{-4}$	$5.45 \times 10^{-9}$	35.3

The enthalpy for the reaction (Eq. 17) seems reasonable when compared with trends of similar Group IV-A oxide reaction enthalpies calculated from data compiled by Drowart and Goldfinger (Ref. 16). The entropy found for Eq. 17 appears to be too high by at least 10 eu when compared with those of similar reactions (Ref. 17). From the JANAF Tables (Ref. 18),  $S_{1500}^\circ = 75.72$ , 63.56, and 30.83 cal/deg-mole for  $\text{SiO}_2(\text{g})$ ,  $\text{SiO}(\text{g})$ , and  $1/2 \text{O}_2$ , respectively. This yields  $\Delta S_{1500}^\circ = 18.7$  eu for the reaction



## REVISED HENRY'S LAW CONSTANT VALUES

Thermodynamic measurements reported during the past 3 years have allowed us to update some of the Henry's law constants reported by Norman (Ref. 19). In particular, we have found that data for zinc were of some minor interest and should be included. We have obtained a better description of the rare earth dioxides, and one description, including data based both on experimental evidence and on estimated values, is available for promethium. The revised Henry's law constant values are reported in Table 9 and a discussion of the individual elements follows:

1. Zinc. Coughlin's values (Ref. 20), which were confirmed by Hoenig (Ref. 21), have been employed. One-half the silicate correction reported in the Henry's law constant report (Ref. 19) was employed. The  $ZnO(c)$  melting point was taken from Schneider (Ref. 22) (2242°K) and the melting entropy was estimated according to Norman's report (Ref. 19).
2. Germanium. While  $GeO_2(g)$  has been found to be stable, its stability reported elsewhere in this report is such that this gaseous species does not become important during fallout formation. No change in the equation is recommended.
3. Arsenic and Antimony. The species  $AsO_2$  and  $SbO_2$  are apparently unimportant (Ref. 1). No change is recommended.
4. Technetium. The estimated technetium trioxide stability was confirmed experimentally (Ref. 23). No change in the equation is recommended.
5. Tellurium. The  $TeO_2$  measurements reported by Staley (Ref. 24) support the values given in the Henry's law report (Ref. 19). However, the

experimental study revealed that the lower oxygen limit suggested in this report was too low. A limit of  $10^{-4}$  atm oxygen is recommended.

6. Cerium, Praseodymium, and Neodymium. Staley and Norman (Ref. 25) have reported the stabilities of rare earth gaseous dioxides. For the Henry's law report, estimates of these stabilities were made. Experimental values have been used to correct the reported Henry's law values (Ref. 19). The trend of the experimental values is toward lower vapor pressures of the rare earth dioxides than are presented in the Henry's law report.
7. Promethium and Samarium. Promethium values were altered in accordance with the Ce, Pr, and Nd data. Samarium was not altered because the projected stability of the dioxide was not sufficient to warrant it.

TABLE 9  
REVISED HENRY'S LAW CONSTANTS

Element	Estimated or Measured Thermodynamic Equations for Fallout Formation	Lower $P_{O_2}$ Limit
Zn	$\log P_{Zn} P_{O_2}^{1/2} / C_{Zn^{++}} = 11.8 - 23,000/T$	-
Ce	$\log P_{CeO_2} / C_{Ce^{+2}} = 7.0 - 35,400/T$	$10^{-8}$
Pr	$\log PrO_2 / C_{Pr^{+3}} P_{O_2}^{1/4} = 5.7 - 33,800/T$	$10^{-4}$
Nd	$\log NdO_2 / C_{Nd^{+3}} P_{O_2}^{1/4} = 7.6 - 35,700/T$	$10^{-4}$
Pm	$\log PmO_2 / C_{Pm^{+3}} P_{O_2}^{1/4} = 7.3 - 37,400/T$	$\sim 10^{-4}$

## RELEASE OF RADIOIODINE BY SIMULATED FALLOUT PARTICLES

The biological availability of radioiodine, as released by fallout particles, is an important part of the fallout problem. A preliminary study of radioiodine airborne release by simulated fallout particles has been completed.

Tellurium dioxide particles with an average "diameter" of 10 micrometers were neutron-irradiated in a G-1 General Atomic TRIGA reactor and then decayed for at least 50 half-lives of Te-131. The particles were then placed in a thermally equilibrated transpiration apparatus, and the released I-131 was gettered in MI-1 charcoal traps. The apparatus is shown in Fig. 11. Oxygen was passed through a humidifier at room temperature and then over the sample, which was contained in a porcelain boat. At various intervals, the traps are removed, replaced with fresh traps, and monitored for the 0.36 MeV radioiodine photopeak. An auxiliary trap of Masalinn cloth was used to establish that the radioiodine had not passed the charcoal getters. At the end of an experiment, the source was removed from the apparatus and analyzed for radioiodine after cooling.

The basic data are shown in Fig. 12 where the ordinates are proportional to the fractional radioiodine release,  $F \times 10^4$ , and the abscissas are the square root of the time,  $\text{min}^{1/2}$ . The data were plotted in this fashion because it was anticipated that the mechanism of radioiodine release might be condensed-state diffusion; i.e., no surface barrier exists. This appears to be the case because of the near linearity of the data plotted in this manner. The fact that some of the curves do not pass through the origin and that some exhibit a lag period or a burst effect is attributed to experimental conditions. However, the fractional release rates at later times are not strongly perturbed by this problem.

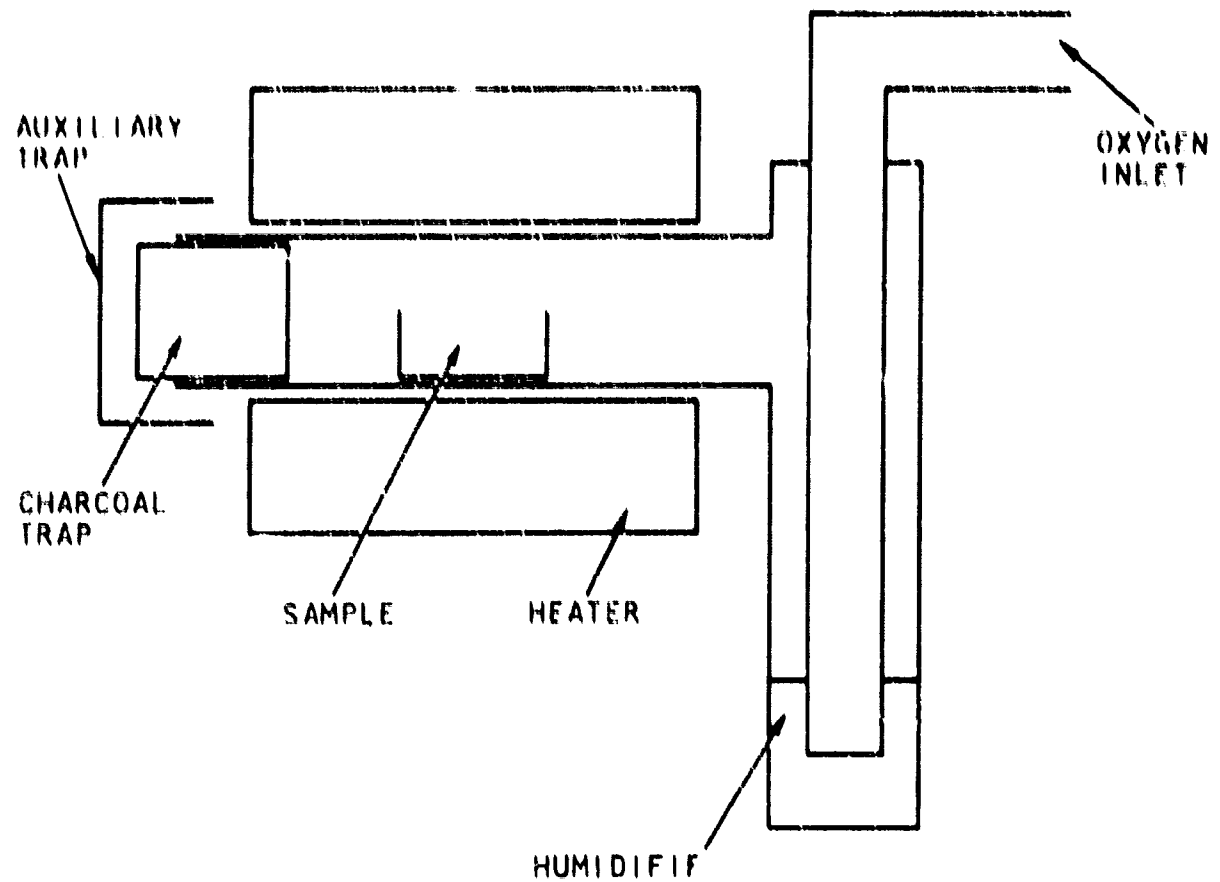


Fig. 11. Apparatus used for monitoring the release of radioiodine by simulated fallout particles

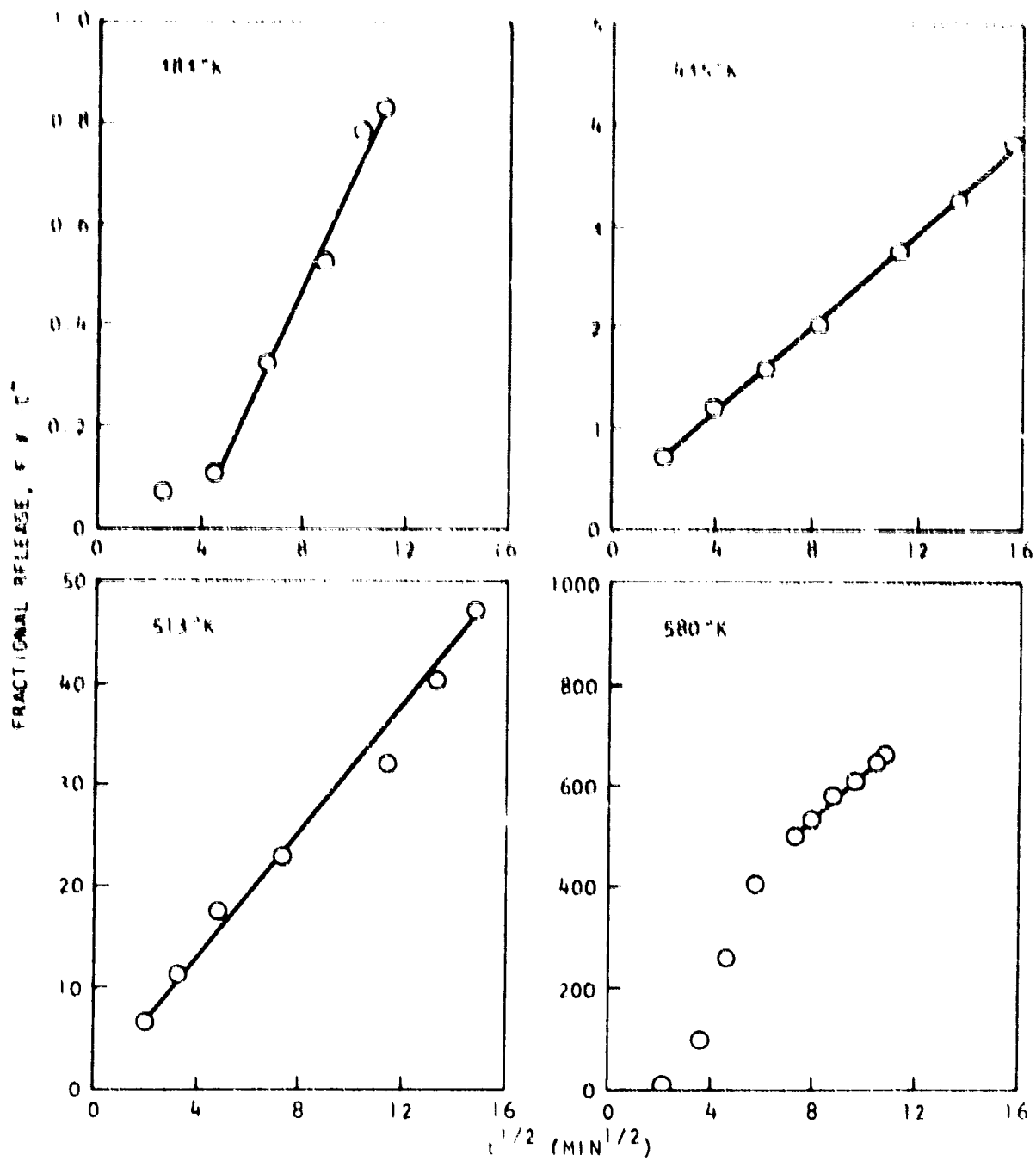


Fig. 12. Fractional release F of I-131 by neutron-irradiated  $\text{TeO}_2$  particles as a function of the square root of the time at four temperatures

It was assumed that condensed-state diffusion was the rate-limiting mechanism in these experiments, and each set of basic data was treated by the method of least squares to obtain the slope of the linear portion of the fractional release as a function of the square root of the time. The equation (Ref. 9)

$$F = (6/R) (Dt/n)^{1/2} \quad (19)$$

was then used to obtain diffusion coefficient values. In Eq. 19, F is the fractional release, R is the particle radius (cm) (it is assumed that all particles were the same size), D is the diffusion coefficient (cm<sup>2</sup>/sec), and t is the time (sec). The resulting diffusion coefficients are listed in Table 10.

TABLE 10  
DIFFUSION COEFFICIENTS FOR RADIOIODINE RELEASE  
BY SIMULATED FALLOUT PARTICLES

T (°K)	log <sub>10</sub> D (D in cm <sup>2</sup> /sec)
383	-19
435	-18
513	-14
580	-13

The results in Table 10 are summarized in Fig. 13 and in Eq. 20:

$$D = 0.605 \exp(-33700/RT) , \quad (20)$$

where R is the gas constant and T is in °K. The line drawn through the points in Fig. 13 was obtained by the method of least squares, and corresponds to Eq. 20. The values in Table 10 have been rounded off because these preliminary data do not warrant closer description. The Arrhenius treatment implies that the radioiodine release is an activated process that is probably condensed-state diffusion limited.

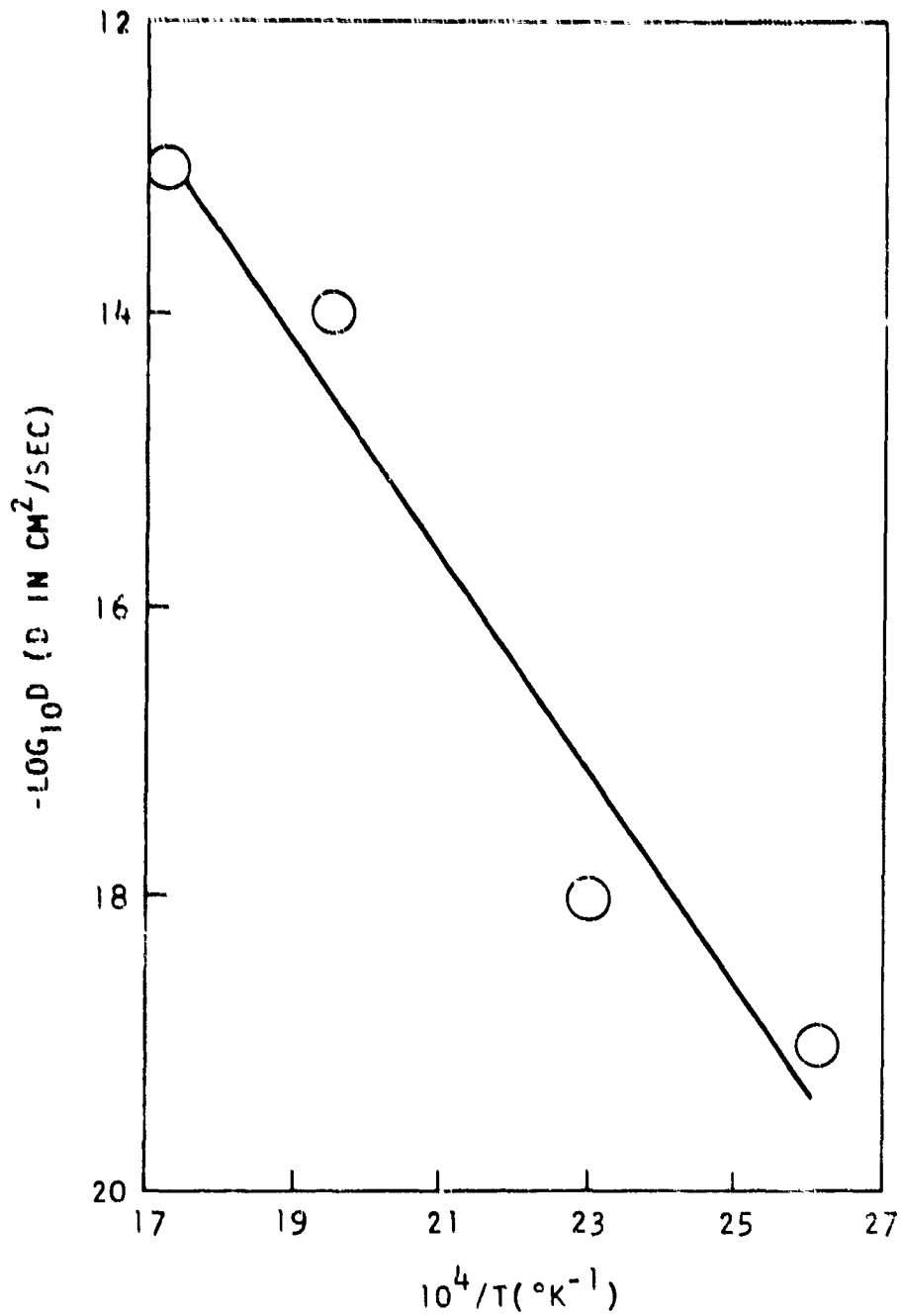


Fig. 13. Dependence of estimated diffusion coefficients upon temperature for release of radioiodine from neutron-irradiated  $\text{TeO}_2$  particles

The low values of the diffusion coefficients would be difficult to measure except that the particle size is sufficiently small to allow measurement. A calculation of the room temperature radioiodine release from a 0.1 micrometer particle of  $\text{TeO}_2$  was made using the results from Eq. 20. This calculation pertains to an atmosphere of oxygen that is assumed to be saturated with water vapor at room temperature. The results of the calculation are shown in Fig. 14, where the temperature was assumed to be 298°K. Since the release calculated from the particle is small, we conclude that the major hazard for vapor release of radioiodine from a particle is the surface-adsorbed portion (i.e., closer to the surface than 0.1 micrometer).

Although fallout particles are not  $\text{TeO}_2$ , the material they are made of probably does not permit iodine diffusion at rates very different from those for  $\text{TeO}_2$ . This study establishes that water-laden oxygen was capable of removing iodine from the surfaces of a  $\text{TeO}_2$  sample faster than iodine can diffuse through the sample. One can extrapolate this finding to fallout particles and suggest that water-laden air will react with surface iodine compounds on fallout particles at this rate or faster. It is proposed therefore that iodine released from fallout particles in short periods of time resides closer than 0.1 micrometer to the surface of the particle and that it is reasonable to expect a considerable release of this surface iodine.

Because the surface release of radioiodine by simulated fallout particles is of considerable interest, another experiment was performed. In this experiment part of the charcoal nearest the I-131 source was replaced with NBS standard glass beads having diameters of 1.17 to 1.65 mm. The radioiodine was deposited on the surfaces of the beads near room temperature. After the system had operated for several hours, the beads and charcoal were gamma analyzed and the beads were found to have adsorbed enough iodine to study its release. The beads were placed in a small flask that was stoppered with a fresh charcoal trap. The release of radioiodine at room temperature in the laboratory atmosphere was then monitored by gamma analyzing the charcoal at various intervals.

The fractional release data are shown in Fig. 15. A least squares

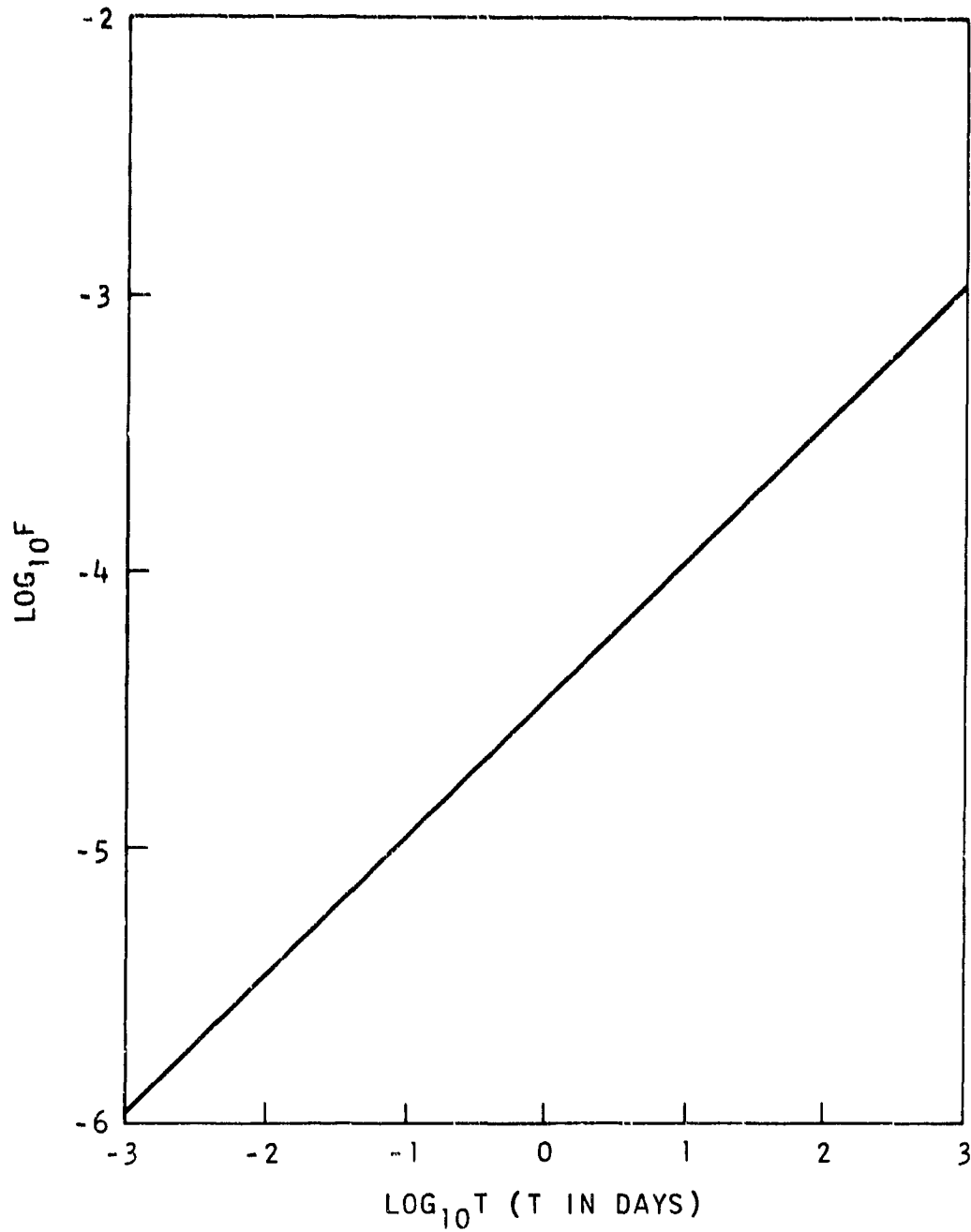


Fig. 14. Calculated fractional release  $F$  of radiiodine by an  $0.1 \mu\text{m}$  particle at  $298^\circ\text{K}$

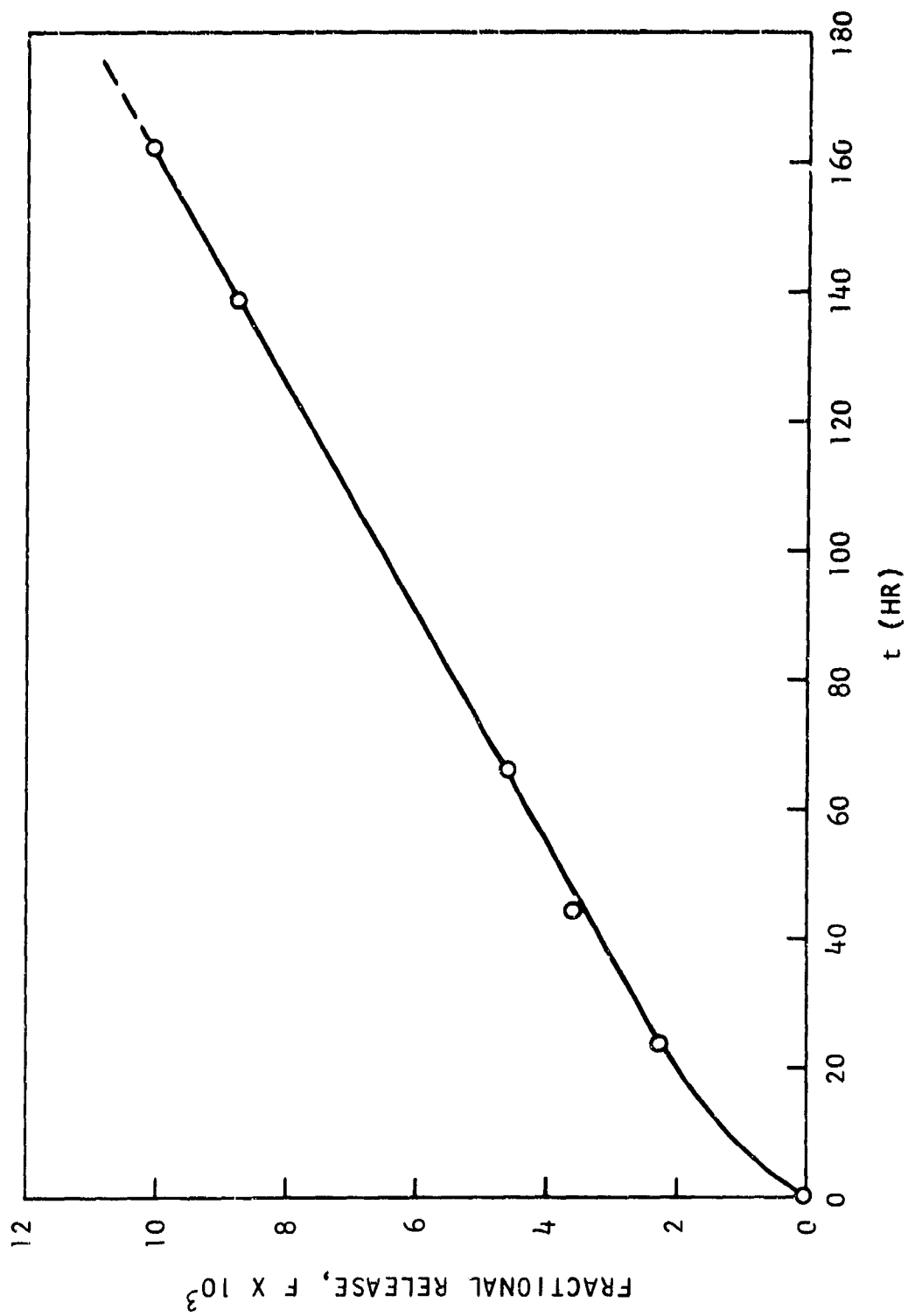


Fig. 15. Fractional release of surface-adsorbed I-131 by glass spheres at 298°K in laboratory air as a function of time

treatment of the data gave

$$F \times 10^3 = 0.945 + 5.58 \times 10^{-2} t , \quad (21)$$

where  $t$  is in hours. The linearity of the data in Fig. 15 indicates that the release mechanism may be Langmuir vaporization or leaching by the laboratory atmosphere. However, there was evidently a small initial rapid release of iodine, as shown in Fig. 15.

It is concluded that appreciable amounts of adsorbed radioiodine may be lost to the atmosphere from fallout particles at room temperature during the half-life of I-131.

This method of radioiodine deposition should prove useful to others involved in the fallout problem. It was noted that MI-1 charcoal is an excellent getter for radioiodine since it retained all of the iodine after 5 hr in one atmosphere of steam in an auxiliary experiment.

Following the air-release experiment, the beads were leached with distilled water. At intervals, a small aliquot was removed, gamma-analyzed, and replaced in the container. A small volume of saturated KI was then introduced, and the leaching was again monitored at various periods. The data are shown in Fig. 16. A solution of KI is obviously a better leaching agent than  $H_2O$ . Most of the sorbed I could be removed with a KI solution.

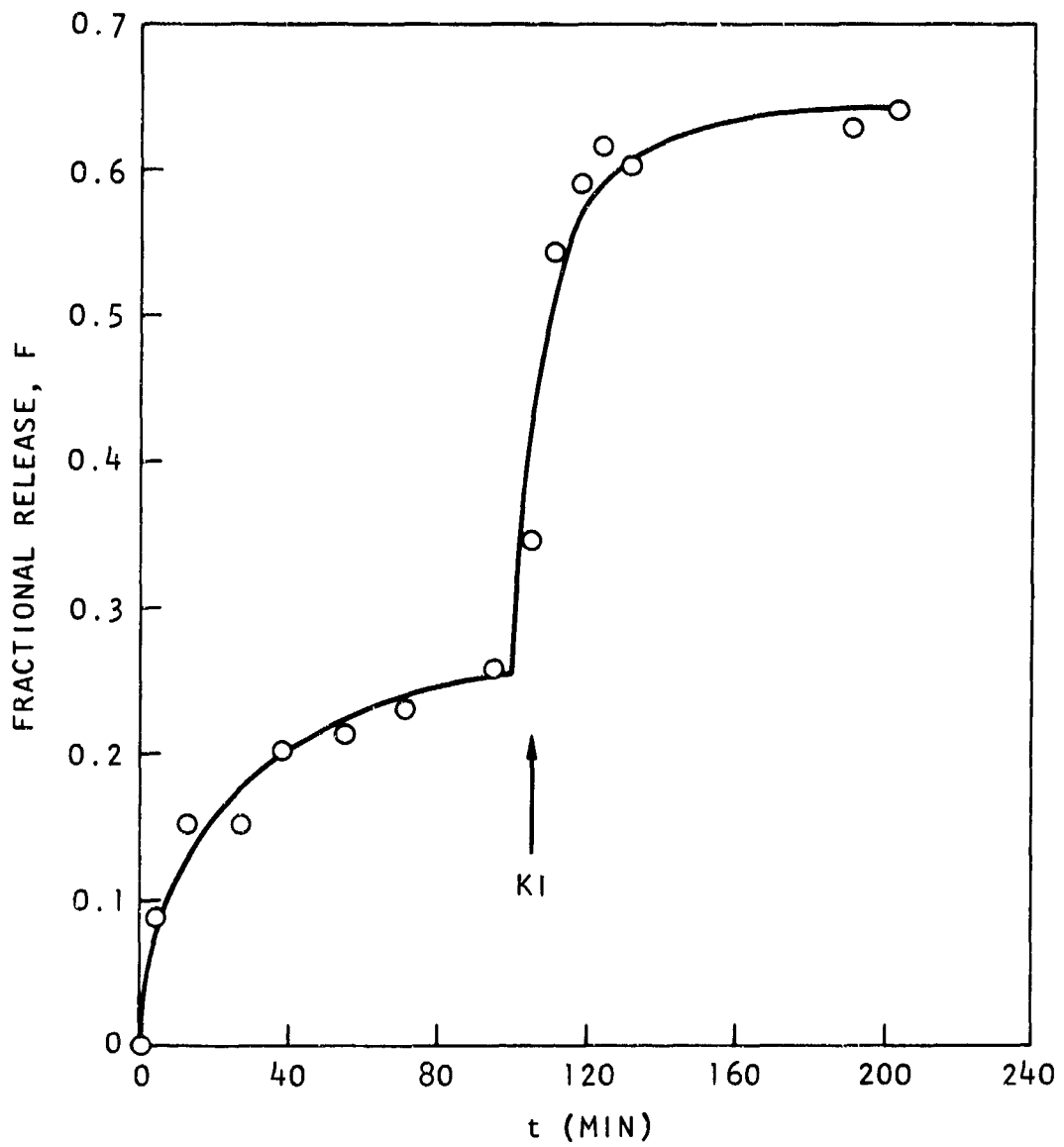


Fig. 16. Leaching of adsorbed I-131 from glass spheres with distilled water and potassium iodide at 298°K as a function of time

## LEACHING STUDIES

The biological availability of fission products is important in any complete description of the fallout problem. The most important single process involved in making fission products available for metabolism is that of leaching of fallout particles by various fluids. A study of this process had been initiated, and some preliminary results are reported here.

Two silicate matrices were used, vitreous Nevada soil (Ref. 1) and a glass of 1175°C eutectic composition from the  $\text{CaO-Al}_2\text{O}_3\text{-SiO}_2$  ternary system (Ref. 1). The glasses were treated by heating them on flat platinum surfaces for several hours at 1400°C in air. Upon cooling, a small piece of enriched-uranium foil was placed between the two flat glass surfaces, and the sample was irradiated with neutrons in a Gulf General Atomic TRIGA reactor for 125 kWh. The radioactivity was allowed to decay for approximately 5 days, after which the glasses were separated from the foil and were lightly cleaned, using fine carborundum paper, to eliminate spalled uranium and fission products from the surfaces. After the samples were cleaned and dried, they were subjected to leaching at room temperature in plastic beakers containing 5 ml of a slurry of 11.5 g of montmorillonite in 750 ml of distilled water. The clay was used to provide an efficient sink for leached fission products. During leaching, both the glasses and the leaching slurries were separately analyzed using a 4096-channel gamma analyzer equipped with a lithium-drifted germanium detector. The gamma spectra were then corrected by referring them to the irradiation time using the pertinent half-lives and a computer. The nuclides that were found in all spectra for the leaching slurries, and for both glasses, are listed in Table 11.

The data are shown in Figs. 17 and 18, where the fractional releases of the glasses are plotted as functions of the square root of the time. From these figures, it appears that the leaching process is one of diffusion

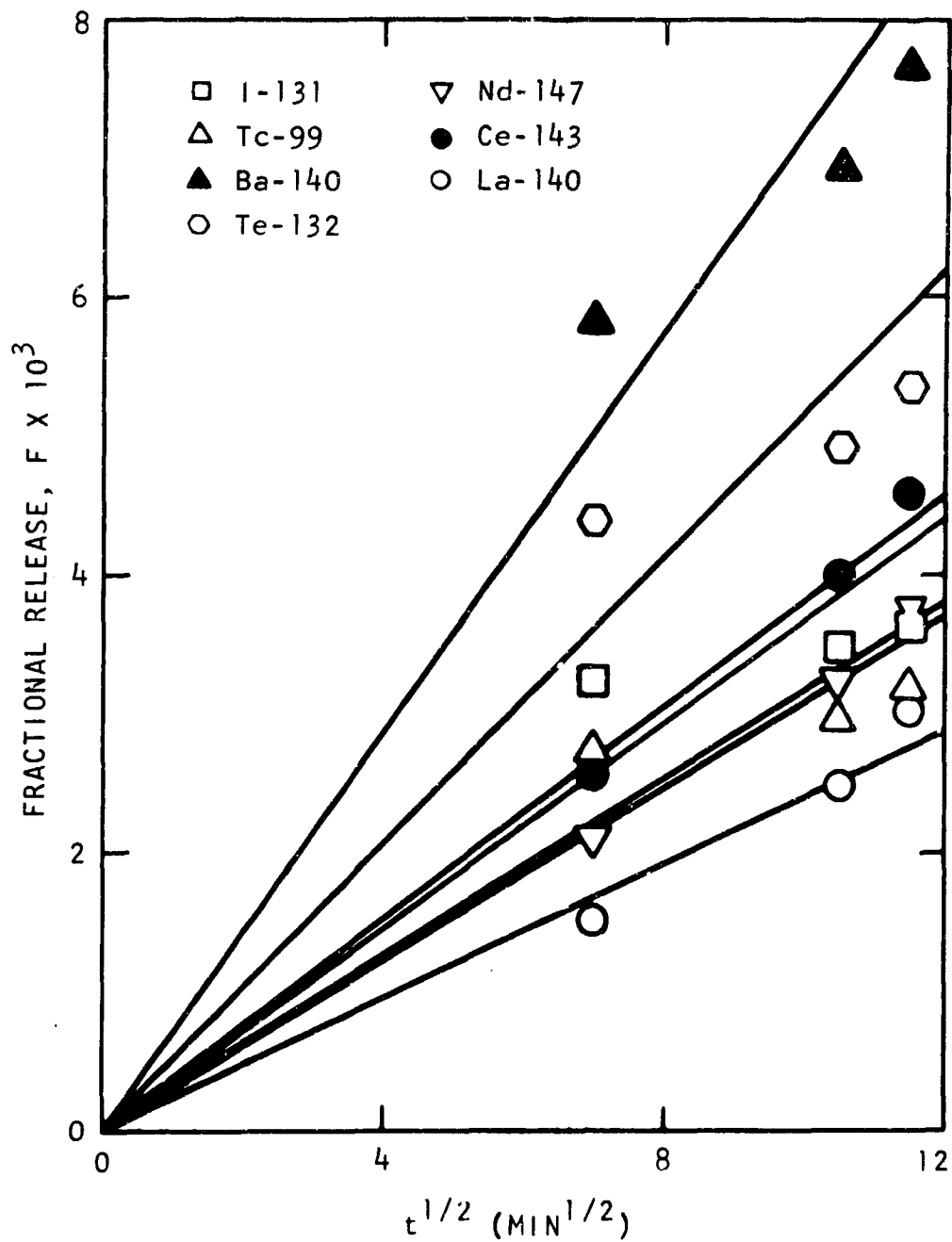


Fig. 17. Fractional release of fission products from eutectic glass during leaching; the average uncertainty is 15%

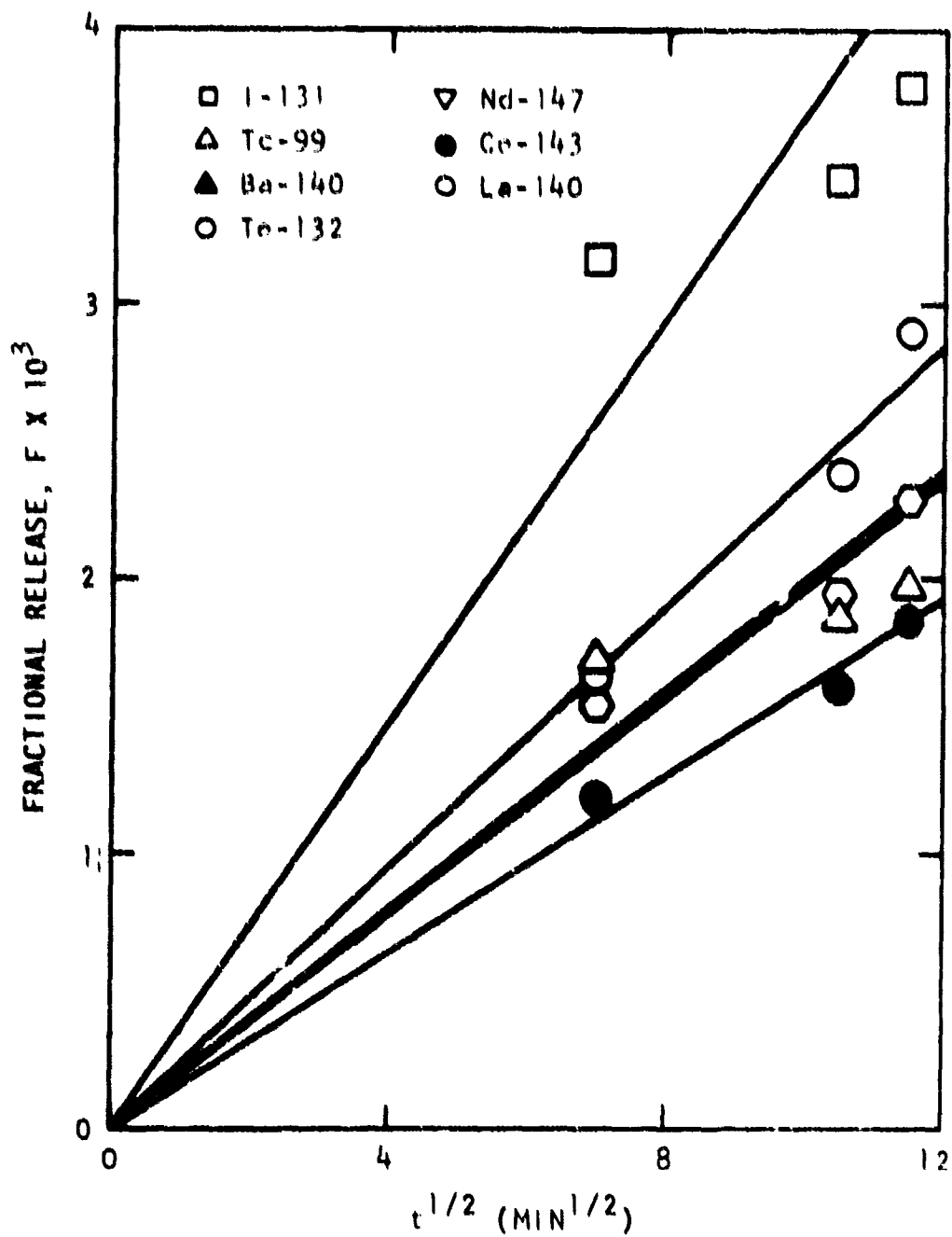


Fig. 18. Fractional release of fission products from Nevada glass during leaching; the average uncertainty is 25%.

during the leaching period of 132 min. Several qualitative conclusions may be made concerning these data. Since the fractional releases are not highly correlated with mass number, the leaching process is not totally dependent upon the recoil distribution of fission products. One may also calculate the approximate leaching penetration during the experiment. Assuming a recoil range of 10 micrometers for a nuclide in the eutectic glass, and using a fractional release value of  $5 \times 10^{-3}$  for this nuclide, a penetration distance of approximately  $200 \text{ \AA}$  is calculated. Thus, the surface orientation of the individual nuclides in fallout will play a dominant role during leaching. In the present study, leaching rates differ by only a factor of about 4 for all the nuclides studied in the two glasses. The reason for differences between nuclides is not known, although, if diffusion is rate-controlling, such differences are expected. It is also observed that the order of leaching rates of different nuclides from the eutectic glass differs from that of the Nevada glass. Also, surprisingly, the leaching rates are only slightly different for the two glasses. This, however, is consistent with the similarity of these two glasses in diffusion studies. Further experiments with these systems are in progress.

TABLE 11  
 RADIONUCLIDES PRESENT IN LEACHING SLURRIES  
 FOR NEVADA AND EUTECTIC GLASSES

Nuclide	$\gamma$ Energy (keV)
Nd-147	91
Tc-99	140
Ce-143	293
Te-132	228
Ba-140	538
La-140	329
La-140	487
I-131	364

## PUBLICATIONS

The papers listed below describe investigations that were completely or partly supported by contracts with the Office of Civil Defense, Office of the Secretary of the Army, and Department of Defense and have been submitted, accepted, or published during the past year. They should be regarded as part of the final report.

Staley, H. G., "A Mass-Spectrometric Knudsen-Cell Study of the Gaseous Oxides of Tellurium," accepted for publication in J. Chem. Phys.

Winchell, P., and J. H. Norman, "A Study of the Diffusion of Radioactive Nuclides in Molten Silicates at High Temperatures," in High Temperature Technology, Proceedings of the Third International Symposium, Asilomar, California, 1967, Butterworths, London, 1969, p. 479.

Winchell, P., "The Compensation Law for Diffusion in Silicates," High Temp. Sci. 1, 200 (1969).

Winchell, P., "The Stokes-Einstein Equation and Molten Silicates," submitted for publication in Phys. Chem. Glasses.

Norman, J. H., P. Winchell, J. M. Dixon, B. W. Roos, and R. F. Korts, "Spheres: Diffusion-Controlled Fission Product Release and Absorption," in Radionuclides in the Environment, Advances in Chemistry Series, No. 93, R. F. Gould (ed.), American Chemical Society, Washington, D.C., 1970, p. 13.

## REFERENCES

1. Norman, J. H., P. Winchell, and H. G. Staley, "Cloud Chemistry of Fallout Formation: Final Report," Office of Civil Defense Report GA-9180, Gulf General Atomic Incorporated, January 31, 1969.
2. Analytical Chemistry of the Manhattan Project, C. J. Rodden, Editor-in-Chief, National Nuclear Energy Series, Manhattan Project Technical Section, Division VIII-Volume 1, McGraw-Hill Book Company, Inc., New York, 1950, pp. 523-535.
3. Alväger, T., R. A. Naumann, R. F. Petry, G. Sidenius, and T. D. Thomas, Phys. Rev. **167**, 1105 (1968).
4. Wilhelmy, J. B., "High-Resolution Gamma and X-Ray Spectroscopy on Unseparated Fission Products," USAEC Report UCRL-18978, University of California Lawrence Radiation Laboratory, 1969.
5. Kochendorfer, D. B., "Calculated Activities of U-235 Fission Products for Very Short Nuclear Operation," U.S. Navy Radiological Laboratory Report USNRDL-TR-757, 1964.
6. Crank, J., The Mathematics of Diffusion, Clarendon Press, Oxford, 1956.
7. Freiling, E. C., "Mass-Transfer Mechanisms in Source-Term Definition," in Radionuclides in the Environment, Advances in Chemistry Series 93, American Chemical Society, Publishers, Washington, D.C., 1970, pp. 1-12.
8. Winchell, P., and J. H. Norman, "A Study of the Diffusion of Radioactive Nuclides in Molten Silicates at High Temperatures," in High Temperature Technology, Proceedings of the Third International Symposium, Asilomar, California, 1967, Butterworths, London, 1969, p. 479.
9. Winchell, P., High Temp. Sci. **1**, 200 (1969).
10. Sobol, S. I., "The Effective Ionic Radii of Elements in Melts and in Solids at High Temperature," in Soviet Research in Glass and Ceramics, Basic Science I, Consultants Bureau, Inc., New York, 1957, p. 139.
11. Eitel, W., Silicate Science, v. II, Glasses, Enamels, Slags; Academic Press, New York, 1965, p. 384.

12. Doremus, R. H., "Diffusion of Gold in a Silicate Glass," in Symposium on Nucleation and Crystallization in Glasses and Melts, M. K. Reser (ed.), The American Ceramic Society, Columbus, 1962, p. 119.
13. King, J. B., and P. J. Koros, "Diffusion in Liquid Silicates," in Conference on the Kinetics of High Temperature Processes, John Wiley and Sons, New York, 1959.
14. Brewer, L., Chem. Rev. 52, 47 (1953).
15. Hildenbrand, D. L., "The Dissociation Energy and Ionization Potential of Silicon Monoxide," Paper No. 99, presented at the Seventeenth Annual Conference on Mass Spectrometry and Allied Topics, Dallas, Texas, May 1969.
16. Drowart, J., and P. Goldfinger, Angew. Chem. 6, 581 (1967).
17. Staley, H. G., and J. H. Norman, Int. J. Mass Spect. Ion Phys. 2, 35 (1969).
18. JANAF Thermochemical Tables, The Dow Chemical Company, Midland, Michigan, 1962.
19. Norman, J. H., "Henry's Law Constants for Dissolution of Fission Products in a Silicate Fallout Particle Matrix," U.S. Naval Radiological Defense Laboratory Report GA-7058, General Dynamics Corporation, General Atomic Division, December 29, 1966.
20. Coughlin, J. P., "Contributions to the Data on Theoretical Metallurgy XII: Heats and Free Energies of Formation of Inorganic Oxides," U.S. Bureau of Mines Bulletin 542, U.S. Government Printing Office, Washington, D.C., 1954.
21. Hoenig, C. L., "Vapor Pressure and Evaporation Coefficient Studies of Stannic Oxide, Zinc Oxide and Beryllium Nitride," USAEC Report UCRL-7521, University of California Lawrence Radiation Laboratory, April 1964.
22. Schneider, S. J., "Compilation of the Melting Points of the Metal Oxides," National Bureau of Standards Monograph 68, October 1963.
23. Norman, J. H., P. Winchell, and H. G. Staley, "Cloud Chemistry of Fallout Formation: Final Report," U.S. Naval Radiological Defense Laboratory Report GA-8472, Gulf General Atomic Incorporated, January 1968.
24. Staley, H. G., Gulf General Atomic Incorporated, "A Mass-Spectrometric Knudsen-Cell Study of the Gaseous Oxides of Tellurium," accepted for publication in J. Chem. Phys.

25. Staley, H. G., and J. H. Norman, Int. J. Mass Spect. Ion Phys. 2, 35  
(1969).

UNCLASSIFIED

Security Classification

DOCUMENT CONTROL DATA - R & D		
<i>(Security classification of title, body of abstract and indexing annotation must be entered when the overall report is classified)</i>		
1. ORIGINATING ACTIVITY (Corporate author) Gulf General Atomic Incorporated San Diego, California		2a. REPORT SECURITY CLASSIFICATION UNCLASSIFIED
		2b. GROUP
3. REPORT TITLE CLOUD CHEMISTRY OF FALLOUT FORMATION - FINAL REPORT		
4. DESCRIPTIVE NOTES (Type of report and inclusive dates)		
5. AUTHOR(S) (First name, middle initial, last name) John H. Norman and Perrin Winchell		
6. REPORT DATE February 15, 1970	7a. TOTAL NO. OF PAGES 63	7b. NO. OF REFS 25
8a. CONTRACT OR GRANT NO. DAHC20-69-C-0138	9a. ORIGINATOR'S REPORT NUMBER(S) GA-9945	
b. PROJECT NO.	9b. OTHER REPORT NO(S) (Any other numbers that may be assigned this report)	
c.		
d.		
10. DISTRIBUTION STATEMENT		
11. SUPPLEMENTARY NOTES	12. SPONSORING MILITARY ACTIVITY Office of Civil Defense Office of the Secretary of the Army Washington, D.C. 20310	
13. ABSTRACT <p>In initial studies of short-lived fission products for use in fallout fractionation models, several known isotopes have been recognized. The observed gamma ray intensities of recognized energies from the double-tape recoil-range measuring system are consistent with expected recoil range variations. It is planned to satisfy a requirement for more intense gamma spectra by moving the recoil fission product source close to the reactor.</p> <p>The interaction between condensation phenomena, gas, and condensed-phase diffusion of fission products during fallout formation has been investigated analytically. Regions of importance of each of these phenomena have been discussed.</p> <p>Further tests of the application of the compensation law to condensed-state diffusion data have been carried out. The compensation law applied well to all silicate systems except those loaded by fission-product recoil.</p> <p>The thermodynamics of <math>\text{GeO}_2(\text{g})</math> have been measured. Attempts to define the stabilities of <math>\text{AsO}_2(\text{g})</math> and <math>\text{SnO}_2(\text{g})</math> have failed because of low stability of these species.</p> <p>Gaseous release of iodine from <math>\text{TeO}_2</math> particles has been shown to be controlled by diffusion in the <math>\text{TeO}_2</math>. Rates of diffusion have been determined. These data indicate that the volatility of iodine from fallout particles could be very high. Leaching studies of recoil loaded fission products are consistent with release of these fission products to the aqueous leaching solution being diffusion controlled. These measurements point out the importance of the distributions of fission products in fallout particles to their biological activities.</p>		

DD FORM 1473  
1 NOV 65UNCLASSIFIED  
Security Classification

14. KEY WORDS	LINK A		LINK B		LINK C	
	ROLE	WT	ROLE	WT	ROLE	WT
Fission-product fractionation Henry's law constant Fission-product absorption Diffusion studies Fallout formation Cloud chemistry High-temperature chemistry Mass spectrometry Short-lived fission products Radioactive half-life studies Fission recoil-range studies Gamma-ray spectrum Molten silicates Compensation law Condensation coefficient Knudsen-Cell Studies Gas leaching Liquid leaching						

CLOUD CHEMISTRY OF FALLOUT FORMATION FINAL REPORT. Unclassified. Office of Civil Defense. February 15, 1970, 72 pp. Contract DAMC20-69-C-0138. Work Unit 3111B. Gulf General Atomic Incorporated, San Diego, Ca.

In initial studies of short-lived fission products for use in fallout fractionation models, several known isotopes have been recognized. The observed gamma ray intensities of recognized energies from the double-tape recoil-range measuring system are consistent with expected recoil range variations. It is planned to satisfy a requirement for more intense gamma spectra by moving the recoil fission product source close to the reactor.

The interaction between condensation phenomena, gas, and condensed-phase diffusion of fission products during fallout formation has been investigated analytically. Regions of importance of each of these phenomena have been discussed.

Further tests of the application of the compensation law to condensed-state diffusion data have been carried out. The compensation law applied well to all silicate systems except those loaded by fission-product recoil.

The thermodynamics of  $\text{CeO}_2(\text{g})$  have been measured. Attempts to define the stabilities of  $\text{AsO}_2(\text{g})$  and  $\text{SnO}_2(\text{g})$  have failed because of low stability of these species.

Gaseous release of iodine from  $\text{TeO}_2$  particles has been shown to be controlled by diffusion in the  $\text{TeO}_2$ . Rates of diffusion have been determined. These data indicate that the volatility of iodine from fallout particles could be very high. Leaching studies of recoil loaded fission products are consistent with release of these fission products to the aqueous leaching solution being diffusion controlled. These measurements point out the importance of the distributions of fission products in fallout particles to their biological activities.

CLOUD CHEMISTRY OF FALLOUT FORMATION FINAL REPORT. Unclassified. Office of Civil Defense. February 15, 1970, 72 pp. Contract DAMC20-69-C-0138. Work Unit 3111B. Gulf General Atomic Incorporated, San Diego, Ca.

In initial studies of short-lived fission products for use in fallout fractionation models, several known isotopes have been recognized. The observed gamma ray intensities of recognized energies from the double-tape recoil-range measuring system are consistent with expected recoil range variations. It is planned to satisfy a requirement for more intense gamma spectra by moving the recoil fission product source close to the reactor.

The interaction between condensation phenomena, gas, and condensed-phase diffusion of fission products during fallout formation has been investigated analytically. Regions of importance of each of these phenomena have been discussed.

Further tests of the application of the compensation law to condensed-state diffusion data have been carried out. The compensation law applied well to all silicate systems except those loaded by fission-product recoil.

The thermodynamics of  $\text{CeO}_2(\text{g})$  have been measured. Attempts to define the stabilities of  $\text{AsO}_2(\text{g})$  and  $\text{SnO}_2(\text{g})$  have failed because of low stability of these species.

Gaseous release of iodine from  $\text{TeO}_2$  particles has been shown to be controlled by diffusion in the  $\text{TeO}_2$ . Rates of diffusion have been determined. These data indicate that the volatility of iodine from fallout particles could be very high. Leaching studies of recoil loaded fission products are consistent with release of these fission products to the aqueous leaching solution being diffusion controlled. These measurements point out the importance of the distributions of fission products in fallout particles to their biological activities.

CLOUD CHEMISTRY OF FALLOUT FORMATION FINAL REPORT. Unclassified. Office of Civil Defense. February 15, 1970, 72 pp. Contract DAMC20-69-C-0138. Work Unit 3111B. Gulf General Atomic Incorporated, San Diego, Ca.

In initial studies of short-lived fission products for use in fallout fractionation models, several known isotopes have been recognized. The observed gamma ray intensities of recognized energies from the double-tape recoil-range measuring system are consistent with expected recoil range variations. It is planned to satisfy a requirement for more intense gamma spectra by moving the recoil fission product source close to the reactor.

The interaction between condensation phenomena, gas, and condensed-phase diffusion of fission products during fallout formation has been investigated analytically. Regions of importance of each of these phenomena have been discussed.

Further tests of the application of the compensation law to condensed-state diffusion data have been carried out. The compensation law applied well to all silicate systems except those loaded by fission-product recoil.

The thermodynamics of  $\text{CeO}_2(\text{g})$  have been measured. Attempts to define the stabilities of  $\text{AsO}_2(\text{g})$  and  $\text{SnO}_2(\text{g})$  have failed because of low stability of these species.

Gaseous release of iodine from  $\text{TeO}_2$  particles has been shown to be controlled by diffusion in the  $\text{TeO}_2$ . Rates of diffusion have been determined. These data indicate that the volatility of iodine from fallout particles could be very high. Leaching studies of recoil loaded fission products are consistent with release of these fission products to the aqueous leaching solution being diffusion controlled. These measurements point out the importance of the distributions of fission products in fallout particles to their biological activities.

CLOUD CHEMISTRY OF FALLOUT FORMATION FINAL REPORT. Unclassified. Office of Civil Defense. February 15, 1970, 72 pp. Contract DAMC20-69-C-0138. Work Unit 3111B. Gulf General Atomic Incorporated, San Diego, Ca.

In initial studies of short-lived fission products for use in fallout fractionation models, several known isotopes have been recognized. The observed gamma ray intensities of recognized energies from the double-tape recoil-range measuring system are consistent with expected recoil range variations. It is planned to satisfy a requirement for more intense gamma spectra by moving the recoil fission product source close to the reactor.

The interaction between condensation phenomena, gas, and condensed-phase diffusion of fission products during fallout formation has been investigated analytically. Regions of importance of each of these phenomena have been discussed.

Further tests of the application of the compensation law to condensed-state diffusion data have been carried out. The compensation law applied well to all silicate systems except those loaded by fission-product recoil.

The thermodynamics of  $\text{CeO}_2(\text{g})$  have been measured. Attempts to define the stabilities of  $\text{AsO}_2(\text{g})$  and  $\text{SnO}_2(\text{g})$  have failed because of low stability of these species.

Gaseous release of iodine from  $\text{TeO}_2$  particles has been shown to be controlled by diffusion in the  $\text{TeO}_2$ . Rates of diffusion have been determined. These data indicate that the volatility of iodine from fallout particles could be very high. Leaching studies of recoil loaded fission products are consistent with release of these fission products to the aqueous leaching solution being diffusion controlled. These measurements point out the importance of the distributions of fission products in fallout particles to their biological activities.